


## Harnessing gold nanomaterials for advanced multicolor colorimetric biosensors in food hazards detection

Follow this and additional works at: <https://www.jfda-online.com/journal>

 Part of the [Food Science Commons](#), [Medicinal Chemistry and Pharmaceutics Commons](#), [Pharmacology Commons](#), and the [Toxicology Commons](#)



This work is licensed under a [Creative Commons Attribution-Noncommercial-No Derivative Works 4.0 License](#).

### Recommended Citation

Xie, Longyingzi; Guo, Chenxi; Yang, Lu; and He, Yue (2024) "Harnessing gold nanomaterials for advanced multicolor colorimetric biosensors in food hazards detection," *Journal of Food and Drug Analysis*: Vol. 32 : Iss. 3 , Article 3. Available at: <https://doi.org/10.38212/2224-6614.3511>

This Review Article is brought to you for free and open access by Journal of Food and Drug Analysis. It has been accepted for inclusion in Journal of Food and Drug Analysis by an authorized editor of Journal of Food and Drug Analysis.

# Harnessing gold nanomaterials for advanced multicolor colorimetric biosensors in food hazards detection

Longyingzi Xie<sup>a,b</sup>, Chenxi Guo<sup>a,b</sup>, Lu Yang<sup>a,b</sup>, Yue He<sup>a,b,\*</sup>

<sup>a</sup> Key Laboratory of Quality and Safety Control of Citrus Fruits, Ministry of Agriculture and Rural Affairs, Southwest University, Chongqing, 400712, PR China

<sup>b</sup> Laboratory of Quality & Safety Risk Assessment for Citrus Products (Chongqing), Ministry of Agriculture and Rural Affairs, Citrus Research Institute, Southwest University, Chongqing, 400712, PR China

## Abstract

Hazards such as pathogenic bacteria, mycotoxins, pesticides, antibiotics, heavy metal ions, *etc.*, cause serious food safety problems worldwide due to their toxicity and frequent contamination. Rapid screening is an effective way for food safety control, which highly relies on the development of sensitive, specific, and convenient detection methods. The multicolor colorimetric biosensors based on gold nanomaterials have evolved into advanced tools for detecting various hazards in food, with intuitive readout. The excellent localized surface plasmon resonance (LSPR) properties of gold nanomaterials enable them to exhibit bright colors when used as chromophores. In addition, the small changes in the morphology of gold nanomaterials can lead to significant changes in the wavelength of the LSPR peak, resulting in vivid color changes. Since the color discrimination ability of the normal human eye is usually superior to the intensity change ability, the way in which different concentrations of targets represent vivid color changes makes it feasible to fabricate sensors with improved accuracy in visual semi-quantitative detection. By combining with various signal amplification strategies, the detection sensitivity of the constructed sensors can be further improved, even reaching the level of pg/mL. In this review, two strategies for changing the morphology of gold nanomaterials in constructing multicolor colorimetric biosensors, namely the etching strategy and the growth strategy were discussed. We also highlight current progress in developing different gold nanomaterial-based multicolor colorimetric biosensors for detecting various hazards in food. The hazards in food samples are classified as pathogens, mycotoxins, indicators of food freshness, pesticides, antibiotics, heavy metal ions, food additives, and hazards from food processing and packaging. The multicolor colorimetric biosensors based on gold nanomaterials represent a promising tool for visual detection of hazardous materials in food.

**Keywords:** Antibody, Aptamer, Food safety, Gold nanomaterials, Multicolor colorimetric detection

## 1. Introduction

Food safety is a global public issue and has attracted increasing attention among people. Monitoring hazardous materials in food is crucial for maintaining human life and health. Common contaminants that pose a threat to food safety include foodborne pathogens, mycotoxins, pesticides, antibiotics, heavy metal ions, food additives, and so on [1]. The consumption of contaminated

food or water can cause foodborne illnesses, which usually have strong toxicity and infectivity. To identify potential risks and ensure food safety, the development of sensitive, selective, low-cost, and convenient rapid detection technologies for hazards in food is crucial.

Among numerous detection techniques, colorimetry has long been the most popular technique due to its intuitive detection results. After direct or indirect interaction between target molecules and

Received 29 February 2024; accepted 27 May 2024.  
Available online 13 September 2024

\* Corresponding author.  
E-mail address: [yuehe@cric.cn](mailto:yuehe@cric.cn) (Y. He).

<https://doi.org/10.38212/2224-6614.3511>

2224-6614/© 2024 Taiwan Food and Drug Administration. This is an open access article under the CC-BY-NC-ND license (<http://creativecommons.org/licenses/by-nc-nd/4.0/>).

chromogenic substances, the color of the detection solution shows obvious color changes, which can be easily observed by the naked eyes or recorded by UV-visible spectroscopy [2]. However, due to the low extinction coefficient exhibited by most organic dyes, colorimetric assays based on traditional organic dyes often have the disadvantage of low sensitivity. Compared with organic dyes, gold nanomaterials display a higher extinction coefficients, approximately 1000 times higher in the visible light region, promoting sensitivity at the nanomolar level (or even lower concentration) [3]. The excellent extinction coefficient of gold nanomaterials is due to the localized surface plasmon resonance (LSPR) caused by free electron oscillations on the metal surface under light irradiation [4]. The wavelength and intensity of the LSPR peak of gold nanomaterials are well regulated by their shape, size, distance, and dielectric environment [5]. As a result, the LSPR peak of gold nanomaterials can be easily tuned from visible light to near-infrared range, accompanied by vivid multicolor changes. The characteristic of gold nanomaterials promotes them a good candidate for developing multicolor colorimetric biosensors. In addition, due to the significant sensitivity of the naked eyes to changes in different colors compared with changes in the same color system (10 million color types *versus* 64 grades), the multicolor colorimetric method based on gold nanomaterials has better visual resolution, resulting in higher accuracy in visual semi-quantitative detection. Therefore, numerous multicolor biosensors based on gold nanomaterials have been constructed for various targets. Over the past decades, we have witnessed the rapid development of multicolor colorimetric biosensors as a thriving research field [6,7].

To the author's knowledge, although there have been several excellent and well-cited reviews [8–14] on the application of colorimetric biosensors based on gold nanomaterials in food hazards detection, most of these reviews focused on aggregation modules or a single type of hazards in food, while the systematic review of multicolor colorimetric biosensors for food hazards based on the growth and etching strategy of gold nanomaterials has rarely been reported. Herein, we summarized two important strategies for changing the morphology of gold nanomaterials, namely etching strategy and growth strategy. In addition, we also discussed the fabrication of multicolor colorimetric biosensors based on gold nanomaterials for the detection of various types of hazards in food (Fig. 1). Moreover, the future perspectives and possible challenges of multicolor colorimetric sensing were also discussed.

We hope that this review can provide a reference source for the further development of new efficient and sensitive multicolor colorimetric biosensors for food safety, and we also hope for their wider application in the food industry.

## 2. Strategies for changing the morphology of gold nanomaterials

Gold nanomaterials, due to their prominent optical properties, have become promising chromophores for constructing multicolor colorimetric biosensors. In the preceding paragraph, we have already mentioned that the LSPR peak of gold nanomaterials is highly sensitive to changes in their morphology. The changes in the morphology lead to a series of vivid color changes, just like a rainbow. At present, the etching strategy and the growth strategy are two effective strategies for changing the morphology of gold nanomaterials. The etching strategy, as the name suggests, involves etching gold nanomaterials to gradually reduce their size. While the growth strategy means to grow gold or other metal materials on the surface of gold nanomaterials, causing the size of the gold nanomaterials to gradually increase. Current papers on constructing multicolor colorimetric biosensors often involve the use of the two strategies described in this section.

### 2.1. Etching strategy

In recent years, multicolor colorimetric methods based on etching strategy have acquired widespread attention due to its simplicity, sensitivity, and practicality. In fact, the etching strategy typically uses oxidants to oxidize  $\text{Au}^0$  in gold nanomaterials into  $\text{Au}^+$  [15]. Some common oxidants such as oxygen ( $\text{O}_2$ ) and hydrogen peroxide ( $\text{H}_2\text{O}_2$ ) exhibit etching ability toward gold nanomaterials in warm water under acidic conditions [16,17]. This chemical etching mode typically requires a long oxidation time of about 12 h, which limits its practical application. On the contrary, for the Fenton reaction, it decomposes  $\text{H}_2\text{O}_2$  disproportionately with  $\text{Fe}^{2+}$  catalyst, producing hydroxyl radicals ( $\cdot\text{OH}$ ) that exhibit stronger oxidation ability than  $\text{H}_2\text{O}_2$ . Therefore, the Fenton reaction can be applied to the efficient etching of various gold nanomaterials. Taking gold nanorods (AuNRs) as an example, the surface of AuNRs synthesized by the classical seed growth method is coated with cetyltrimethylammonium bromide (CTAB), which is denser on the side face than on the ends. And oxidants are more likely to come into contact with the



Fig. 1. Overview of the two important strategies for changing the morphology of gold nanomaterials and applications of multicolor colorimetric biosensors based on gold nanomaterials in the field of food hazards detection.

ends of AuNRs that contain less CTAB, causing the ends of the AuNRs to gradually oxidize, ultimately leading to shorter AuNRs [18]. The decrease in aspect ratio of AuNRs leads to a blue shift in the longitudinal band of AuNRs, accompanied by a significant change in solution color. For example, by combining  $\text{H}_2\text{O}_2\text{-Fe}^{2+}$ -mediated AuNRs etching strategy with the catalase-like activity of platinum nanoparticles (PtNPs), a powerful multicolor colorimetric platform was constructed for the detection of silver ions ( $\text{Ag}^+$ ) (Fig. 2A) [19]. In addition, iodine ( $\text{I}_2$ ) with high oxidation ability can also etch gold nanomaterials. The whole process can be completed at  $50\text{ }^\circ\text{C}$  for 15 min. Among the various gold nanomaterials, gold nanostars (AuNSs) are a typical anisotropic gold nanomaterial with highly active tips due to their high surface energy [20]. Therefore,  $\text{I}_2$  can etch their tips easily, leading to a blue shift of the LSPR peak, accompanied by a change in solution color. Based on this, Lu and co-workers [21]

fabricated a multicolor immunoassay method for zearalenone (ZEN) detection by using poly-horse-radish peroxidase (HRP) to catalyze iodide ( $\text{I}^-$ ) into  $\text{I}_2$ , which mediated the etching of AuNSs effectively, achieving a visual limit of detection (LOD) as low as  $0.10\text{ ng/mL}$  (Fig. 2B). Moreover, 3,3',5,5'-tetramethylbenzidine (TMB), commonly used as a commercial substrate in enzyme-linked immunosorbent assay (ELISA), is oxidized to blue ( $\text{TMB}^+$ ) under the catalysis of HRP and further turns yellow ( $\text{TMB}^{2+}$ ) in acidic environments. It's well known that the yellow solution of  $\text{TMB}^{2+}$  enable naked-eye inspection. It is interesting that  $\text{TMB}^{2+}$  also has high oxidizing ability, so it can be used to generate signal changes based on redox reaction to meet the needs of etching-based multicolor colorimetric biosensor fabrication [22]. It should be noted that this multicolor ELISA is performed directly by adding gold nanomaterials to the traditional ELISA.  $\text{TMB}^{2+}$  has the ability to etch gold nanomaterials ( $\sim 90\text{ s}$ ) rapidly,

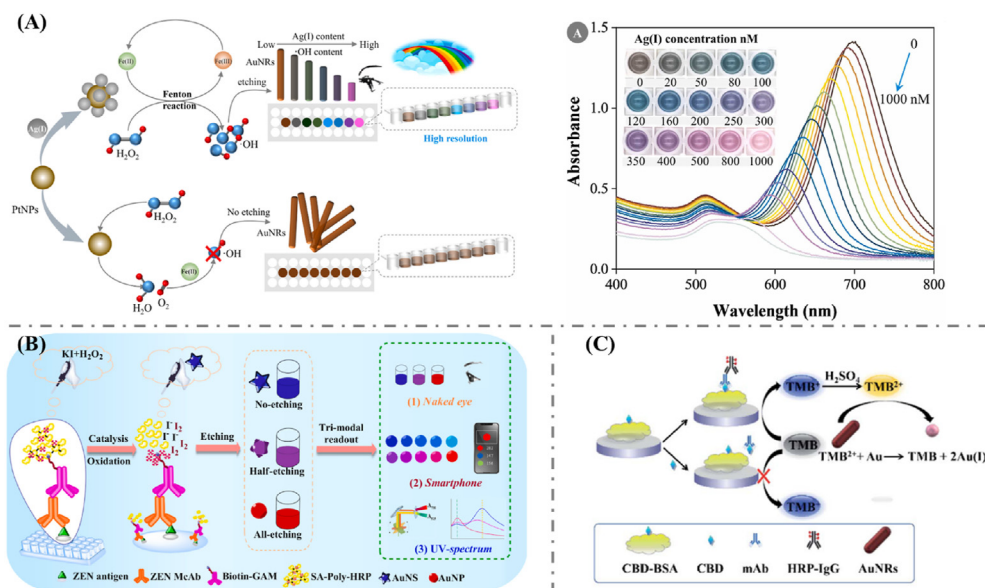


Fig. 2. (A) Schematic illustration of the multicolor colorimetric sensor for Ag<sup>+</sup> based on the etching of AuNRs by •OH (left), and LSPR spectra of AuNRs solution in response to varied Ag<sup>+</sup> concentrations (inset: corresponding images) (right). Reproduced with permission from Ref. [19]. (B) Schematic illustration of the multicolor colorimetric ELISA for ZEN based on the etching of AuNSs by I<sub>2</sub>. Reproduced with permission from Ref. [21]. (C) Schematic illustration of the multicolor colorimetric ELISA for CBD based on the etching of AuNRs by TMB<sup>2+</sup>. Reproduced with permission from Ref. [23].

enabling fast multicolor colorimetric detection of target molecules. For example, our group [23] developed a high-resolution multicolor ELISA based on this strategy to detect carbendazim (CBD) (Fig. 2C), achieving a visual LOD of 0.49 ng/mL.

## 2.2. Growth strategy

The second strategy to change the morphology of gold nanomaterials is growth strategy, including heteroepitaxial growth and homoepitaxial growth. The heteroepitaxial growth of gold nanomaterials results in the formation of core-shell nanostructures. In the traditional seed-mediated preparation of gold nanomaterials, ascorbic acid (AA) plays a crucial role. On the one hand, it acts as a reducing agent to promote the growth of gold nanomaterials; On the other hand, its concentration affects the final morphology of the as-prepared materials [24]. Alkaline phosphatase (ALP) is a commonly used commercial enzyme in ELISA, which has the ability to catalyze the hydrolysis of ascorbic acid 2-phosphate (AAP) to AA. The generated AA reduces Ag<sup>+</sup> to Ag<sup>0</sup> slowly, forming a silver shell on gold nanomaterials. This process, also known as enzymatic metallization [25–27]. The high-resolution color change caused by ALP-mediated metallization can be easily combined with traditional ALP-ELISA to construct multicolor colorimetric biosensors for detecting various targets. For instance, Ma and

co-workers [28] developed a high-resolution multicolor ELISA based on this strategy to detect ZEN. Compared with the traditional ELISA for ZEN, the visual multicolor ELISA was more suitable for rapid screening of a large number of contaminated samples. In addition, urease can also mediate the reduction of Ag<sup>+</sup> to Ag<sup>0</sup>. For example, Pei et al. [29] developed a multicolor ELISA utilizing the strategy of urease-mediated metallization of gold nanoflowers (AuNFs) to visually measure ochratoxin A (OTA) (Fig. 3A). In the presence of urease, urea was hydrolyzed into ammonia, causing Ag<sup>+</sup> to be reduced by the formyl group in glucose. The formed solid Ag<sup>0</sup> is physically adsorbed on the surface of the petals of AuNFs, ultimately forming a silver shell on the surface of AuNFs. With increasing thickness of the silver shell, the shape of AuNFs changes from flowers to spheres, resulting in a blue shift in their LSPR peak and multi-color changes. Given the superior stability of glucose in comparison to previously reported reducing agents, this multicolor ELISA has significant advantages in detecting OTA in real samples. Moreover, beta-galactosidase (β-gal) [30], as a species specific enzymes of *Escherichia coli* (*E. coli*), can catalyze the hydrolysis of *p*-aminophenyl β-D-galactopyranoside to *p*-aminophenol, which also has the reduction ability to induce the formation a silver shell on gold nanomaterials. Taking AuNRs as an example, as single crystal AuNRs, according to the principles of

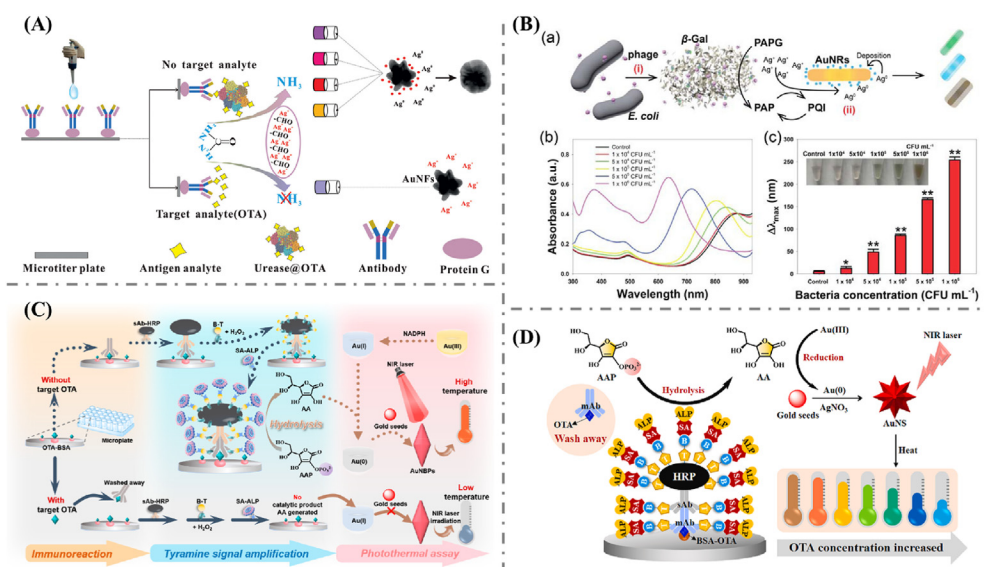


Fig. 3. (A) Schematic illustration of the multicolor colorimetric ELISA for OTA based on urease-mediated metallization of AuNFs. Reproduced with permission from Ref. [29]. (B) Schematic illustration of the multicolor colorimetric biosensor for  $\beta$ -gal in *E. coli* based on  $\beta$ -gal-mediated metallization of AuNRs (a), LSPR spectra of the AuNRs solution in response to different *E. coli* concentrations (b), and LSPR peak shift of the AuNRs in the presence of different concentration of *E. coli* (inset: corresponding images) (c). Reproduced with permission from Ref. [33]. (C) Schematic illustration of the multicolor colorimetric ELISA for OTA based on ALP-mediated in situ growth of AuNBPs. Reproduced with permission from Ref. [37]. (D) Schematic illustration of the multicolor colorimetric ELISA for OTA based on ALP-mediated in situ growth of AuNSs. Reproduced with permission from Ref. [36].

crystallography, epitaxial growth of silver on AuNRs mainly occurs on the lateral facets in the short-axis direction [31,32]. This growth results in a decrease in aspect ratio of AuNRs, which in turn causes a blue shift in the longitudinal LSPR peak of AuNRs. Based on this feature, Chen et al. [33] developed a multicolor colorimetric biosensor for the detection of *E. coli* in resource-constrained settings (Fig. 3B).

The homoepitaxial growth strategy, also known as seed-mediated *in situ* growth strategy. The mechanism of homoepitaxial growth strategy is the reduction of gold ions, which then deposit on the gold seeds for growth. This homoepitaxial growth strategy, also commonly known as *in situ* growth strategy, can nicely control the morphology of gold nanomaterials through several key factors. They are the shape of the seeds, the relative concentration of gold ions/silver nitrate/ascorbic acid, the pH of the growth solution, the concentration of surfactants, and the concentration of halide counterions [24,34,35]. Our group reported that the *in situ* growth of AuNSs and gold nanobipyramids (AuNBPs) mediated by ALP was highly suitable for constructing multicolor ELISA platforms [36,37]. The secondary antibody-labeled ALP catalyzed the hydrolysis of AAP to AA, thus inducing the reduction of gold ion to Au<sup>0</sup>, and then depositing Au<sup>0</sup> on the gold seeds for growth. As for the growth of AuNSs, the entire process can be quickly completed within 5 s at room

temperature [38]. For the growth of AuNBPs, the entire process takes longer (15 min), and the temperature required for growth is also higher (55 °C). Nevertheless, the as-prepared AuNBPs with narrow size distribution resulted in rich color changes responsive to different concentrations of OTA. Compared with the growth strategy of AuNSs, the *in situ* growth of AuNBPs-based multicolor ELISA displayed better sensitivity (Fig. 3C and D).

### 3. Detection of food hazards

Owing to the extraordinary advantages and excellent performance of multicolor colorimetric biosensors based on gold nanomaterials, multicolor colorimetric detection technology has begun to flourish in the field of rapid detection for food safety, and more robust multicolor colorimetric methods have been developed and applied to real food samples. Common food hazards can be roughly divided into pathogens, mycotoxins, indicators of food freshness, pesticides, antibiotics, heavy metal ions, food additives, and hazards from food processing and packaging, as summarized below.

#### 3.1. Pathogens

Foodborne pathogen infection is the main factor leading to foodborne diseases and has been

recognized as a major threat to global public health. Common foodborne pathogens, such as *Staphylococcus aureus* (*S. aureus*), *Salmonella typhimurium*, *Salmonella enterica Choleraesuis* (*S. Choleraesuis*), *E. coli* O157:H7 (*E. coli* O157:H7), *Listeria monocytogenes* (*L. monocytogenes*), *Vibrio parahaemolyticus* (*V. parahaemolyticus*), and *Shigella Bogdii* are widely present in food and food production processes. Among various pathogens detection methods developed in the past, multicolor colorimetric sensors stand out for their ease of operation, high sensitivity, and intuitive signal readout.

The determination of species-specific enzymes refers to a prominent approach for large-scale screening of foodborne pathogens. For example,  $\beta$ -gal produced by *E. coli* has been widely used to determine the concentration of *E. coli*. Zhou et al. [30] developed a highly sensitive and convenient multicolor colorimetric method for the detection of  $\beta$ -gal and *E. coli*. This method was based on  $\beta$ -gal-mediated cascade reactions to regulate the etching of AuNRs, thus significantly improved sensitivity and achieved high-resolution visual detection. Since this method does not require any cell permeabilization, lysis, or centrifugation, it significantly shortens the analysis time for *E. coli*, and therefore has the advantage of being easy to operate. The detection range of this method for *E. coli* was  $1.0 \times 10^2$  to  $1.0 \times 10^5$  CFU/mL with a LOD as low as 22 CFU/mL. Its high accuracy has been proved in real-world tests of orange juice, apple juice, peach juice, grape juice, urine, and river water, demonstrating its potential applications in different environments. Later, Zhou et al. [39] developed another highly sensitive multicolor colorimetric method for the detection of micrococcal nuclease (MNase) to reflect the concentration of *S. aureus*. Vivid color changes in response to different concentrations of *S. aureus* were obtained through ALP mediated metallization of AuNRs. Interestingly, the dual enzyme signal amplification system composed of MNase and ALP significantly improved detection sensitivity and achieved a visual LOD of 25 CFU/mL. Its high accuracy has also been proved in real-world tests of milk, urine, and river water. The above results indicate that the development of multicolor biosensors based on species-specific enzymes is a very promising approach for rapid detection of foodborne pathogens.

In addition, it should be noted that the resistance of pathogenic bacteria to antibiotic poses a serious threat to public health [40]. For example, the occurrence and prevalence of methicillin-resistant *S. aureus* have led to severe bacterial infections, causing hundreds of millions of hospitalizations and deaths worldwide each year. Due to the fact that the

*mecA* gene is an indicator of methicillin-resistant *S. aureus*, the development of early diagnostic methods for the *mecA* gene is of great significance for the prevention and treatment of methicillin-resistant *S. aureus* infection. In response to this goal, Zhou et al. [41] reported a multicolor and ultrasensitive colorimetric method for the detection of *mecA* gene of *S. aureus* in milk (Fig. 4A). Rainbow-like color changes related to different concentrations of target DNA were obtained through the strategy of ALP-mediated *in situ* growth of AuNBPs. Due to the design of multiple hybridization chain reactions (HCRs) on AuNPs, this method achieved a low LOD of 2.71 pM for target DNA.

Moreover, various advanced multicolor colorimetric biosensors based on antibody recognition and aptamer recognition have been constructed for the detection of foodborne pathogens. For example, Gao et al. [42] developed a multicolor ELISA using antibody as recognition element for the sensitive detection of *S. Choleraesuis* in milk. The rich color changes came from the metallization of AuNRs mediated by urease labeled on the detection antibody. Under optimized conditions, the visual LOD of this method was  $1.21 \times 10^2$  CFU/mL. As a new type of recognition element that can also bind targets with high affinity and selectivity, aptamers have attracted increasing interest [43]. Compared with antibodies, they have advantages in high stability, easy modification, simple preparation, and low cost. Liu et al. [44] developed another multicolor colorimetric biosensor using both aptamer and antibody as recognition elements for the sensitive detection of *L. monocytogenes* in pork. They modified aptamer and antibody on magnetic beads (MBs) and manganese dioxide nanoparticles (MnO<sub>2</sub> NPs), respectively. After the formation of aptamer-*L. monocytogenes*-antibody complexes and magnetic separation, MnO<sub>2</sub> NPs with oxidase activity catalyzed the production of TMB<sup>2+</sup>, which effectively etched AuNRs, leading to vivid color changes corresponding to different concentrations of *L. monocytogenes*. The visual LOD of this method was as low as 10 CFU/mL. To further reduce the operational steps and detection time, multifunctional nanomaterials with both magnetic and catalytic properties were synthesized. It is interesting that the binding event between target bacteria and recognition elements labeled on multifunctional nanomaterials significantly reduces the catalytic ability of multifunctional nanomaterials. Based on this principle, Liu et al. [45] proposed a novel sensitive multi-colorimetric method for the detection of *S. aureus*. Fe<sub>3</sub>O<sub>4</sub>-Ag-MnO<sub>2</sub> with both magnetic property and oxidase-like activity was labelled with antibody for the specific detection of *S. aureus* in milk and

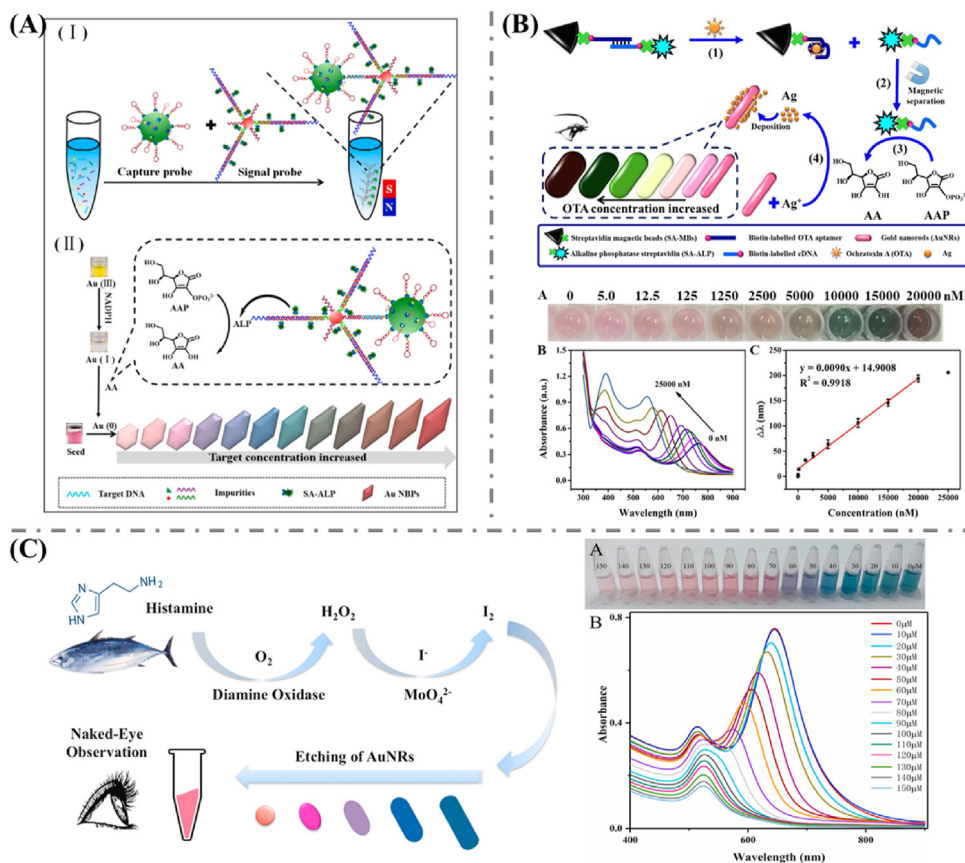


Fig. 4. Multicolor colorimetric sensors for the detection of biological food hazards. (A) Schematic illustration of the multicolor colorimetric biosensor for the detection of *mecA* gene in *S. aureus* based on the signal amplification of multi-HCR on AuNPs and ALP-mediated in-situ growth of AuNBPs. Reproduced with permission from Ref. [41]. (B) Schematic illustration of the multicolor colorimetric aptasensor for visually detecting OTA through ALP-mediated metallization of AuNRs (upper), and images and LSPR spectra of the detection solution in response to different OTA concentrations (lower). Reproduced with permission from Ref. [53]. (C) Schematic illustration of the multicolor colorimetric biosensor for histamine based on the etching of AuNRs by  $I_2$  (left), and images and LSPR spectra of the detection solution in response to varied concentration of histamine (right). Reproduced with permission from Ref. [60].

pork. The binding of  $Fe_3O_4$ -Ag-MnO<sub>2</sub>-antibody complexes to *S. aureus* inhibited the oxidase-like activity of  $Fe_3O_4$ -Ag-MnO<sub>2</sub>, resulting in a decrease in TMB<sup>2+</sup> production and ultimately effectively inhibiting the etching of AuNRs. The visual LOD of *S. aureus* was 10 CFU/mL. Similarly, by using aptamer as recognition element, Zhang et al. [46] constructed another multicolor colorimetric method based on  $Fe_3O_4$ /MnO<sub>2</sub> for the detection of *S. aureus*, *L. monocytogenes*, *E. coli* O157:H7 and *V. parahaemolyticus*, respectively. This method was validated for each of the four bacterial species mentioned above, with a visual LOD 10 CFU/mL. In particular, the entire process only took 40 min and can be applied to pork samples.

### 3.2. Mycotoxins

Mycotoxins are toxic compounds produced as secondary metabolites by various fungi, posing

significant risks to the health of both humans and animals. These toxins are pervasive in a wide array of food products and animal feeds, leading to potential bioaccumulation in the human body through dietary consumption. Notable mycotoxins such as aflatoxins (AFs), OTA, and deoxynivalenol (DON) have been identified as potential carcinogens and can cause acute illnesses at elevated levels [47]. The positive public awareness highlights the importance of mycotoxin screening in protecting the health of global consumers.

To address this challenge, Ma et al. [48] first developed a multicolor colorimetric ELISA based on AuNRs for point-of-care detection of aflatoxin B1 (AFB1) with the naked eyes. AFB1 in the test sample competed with catalase-AFB1 to bind to the antibody of AFB1 captured on the microplate. In the absence of AFB1, catalase-AFB1 was captured on the microplate through the binding reaction between catalase-AFB1 and antibody of AFB1. Then, catalase



captured on the microplate catalyzed the hydrolysis of  $\text{H}_2\text{O}_2$ , thereby preventing the Fenton reaction between  $\text{H}_2\text{O}_2$  and  $\text{Fe}^{2+}$ , ultimately resulting in AuNRs not being etched. However, in the presence of AFB1, catalase-AFB1 captured on the microplate was reduced, resulting in a decrease in the decomposition of  $\text{H}_2\text{O}_2$ . The Fenton reaction between the remaining  $\text{H}_2\text{O}_2$  and  $\text{Fe}^{2+}$  generated free radicals of  $\cdot\text{OH}$ , thereby leading to the etching of AuNRs. Therefore, the longitudinal LSPR peak shift of AuNRs was proportional to AFB1 concentration. This method achieved visually determining AFB1 level as low as 0.12 ng/mL in rice, demonstrating its high feasibility. To further improve the sensitivity, Xiong et al. [15] developed a dual enzyme cascade catalytic reaction to mediated the etching of AuNRs. The cascade reaction was initiated by converting glucose into gluconic acid and  $\text{H}_2\text{O}_2$  through glucose oxidase. Subsequently, HRP catalyzed  $\text{H}_2\text{O}_2$  to produce  $\cdot\text{OH}$ , which led to the etching of AuNRs. The cascade reaction greatly amplified the detection signal, thereby significantly improving the detection sensitivity, achieving a visual LOD of 12.5 pg/mL. These results indicate that this multicolor colorimetric ELISA provides a promising platform for high-sensitivity detection of AFB1 in corn samples. Recently, with the rapid development of nanotechnology, nanozymes have opened up new possibilities for their wide application and commercialization due to their ease of synthesis, low cost, high stability, and high enzyme-like activity [49]. Zhu et al. [50] synthesized peroxidase like nanozymes, namely  $\text{Cu}_2\text{O}@\text{Fe}(\text{OH})_3$  yolk-shell nanocages, to mediate the etching of AuNRs. More interestingly, this method also achieved ratiometric fluorescence detection of OTA. This dual signal readout mode improved the accuracy of the detection results. In addition, compared with microplates, MBs with high specific surface area have lower steric hindrance in immunoreactions. Based on this feature, He et al. [51] constructed a multicolor colorimetric immunoassay method on MBs for the sensitive detection of AFB1. AFB1-bovine serum albumin (BSA) was first labelled on the surface of MBs. Then, the metallization mediated by secondary antibody-ALP produced a silver shell on AuNRs, causing a blue shift in the longitudinal LSPR peak of AuNRs, accompanied by significant color changes. This method not only had high sensitivity (LOD = 5.7 pg/mL), but also achieved the detection of AFB1 in wheat. The above multicolor colorimetric immunoassays provide a new opportunity for convenient screening of food contamination, as they can achieve intuitive visual detection without complex instruments.

Yu et al. [52] for the first time utilized aptamer as recognition element to develop a multicolor colorimetric biosensor for OTA visual detection. An oligonucleotide sequence composed of OTA aptamer and hemin aptamer was designed. The absence of OTA induced the designed oligonucleotide to be digested by exonuclease I (Exo I). However, when OTA bond to its aptamer, it caused a conformational change in the aptamer, and the resulting steric hindrance effect hindered the Exo I mediated hydrolysis reaction. Subsequently, hemin bond to its aptamer to form DNAzyme with peroxidase like activity, which catalyzed the oxidation of TMB to  $\text{TMB}^{2+}$ . The obtained  $\text{TMB}^{2+}$  mediated etching of AuNRs. Finally, a multicolor aptasensor for OTA visual detection was constructed with a detection limit of 30 nM. Tian et al. [53] developed another multicolor colorimetric aptasensor for visual detection for OTA using the strategy of ALP-mediated metallization of AuNRs (Fig. 4B). This method was suitable for rapid detection of OTA in grape juice, with a LOD of 9 nM. Collectively, multicolor colorimetric assays based on AuNRs have great potential for rapid detection of mycotoxins with the naked eyes in low-resource settings.

In addition, AuNBPs with tip structures have attracted intensive interest due to their lower energy wavelength, narrower plasmon line width, higher extinction cross section, and higher sensitivity to the refractive index. These characteristics render AuNBPs an excellent chromogenic substrate for developing multicolor colorimetric biosensors capable of detecting a wide range of targets. For example, by using AuNBPs as chromogenic substrate, Wei et al. [54] developed a sensitive multicolor colorimetric ELISA for the detection of ochratoxins. In this method, nanoliposomes were used to carry secondary antibodies and HRP, greatly amplifying the response of detection signals to target molecules. The mechanism of this method was to use HRP to catalyze  $\text{H}_2\text{O}_2$  to produce  $\cdot\text{OH}$ , which etched AuNBPs, accompanying with various color changes. Zhang et al. [55] developed another multicolor colorimetric ELISA for visual detection of ZEN in cornmeal samples based on HRP-mediated  $\text{TMB}^{2+}$  production, followed by  $\text{TMB}^{2+}$ -mediated etching of AuNBPs. To reduce tedious manual operations, Guo et al. [56] labeled antibodies against DON on MBs and labeled antigens on HRPs. This method achieves automatic simultaneous detection of 24 samples within 40 min, making it a reliable platform for large-scale DON screening. Furthermore, Zhu et al. [57] synthesized  $\text{Cu}_2\text{O}$  NPs and labeled them with secondary antibodies to fabricate a strategy of nanozyme-mediated etching of

AuNBPs. In this strategy, the as-synthesized  $\text{Cu}_2\text{O}$  exhibited peroxidase like activity, which may overcome the drawbacks of proteases such as poor stability, expensive prices, *etc.* Notably, its LOD for OTA in millet samples was 0.47 ng/L, which was particularly suitable for on-site contamination monitoring.

### 3.3. Indicators of food freshness

Food spoilage could cause significant economic losses and lead to serious food safety issues. Therefore, food freshness is one of the most concerned issues for consumers and the food industry [58]. Many substances can be used as indicators of food spoilage. Among them, biogenic amines can be used as a primary freshness indicator of food, which are produced by the decarboxylation of amino acids during food spoilage caused by microbial activities or endogenous tissue metabolism. The typical biogenic amines produced during food spoilage process includes histamine, putrescine, cadaverine, spermine, spermidine, tyramine, and tryptamine [59]. Therefore, the establishment of simple, convenient, and effective biogenic amines detection methods for evaluating food freshness is crucial for food safety.

Xu et al. [60] first developed a multicolor colorimetric biosensor for rapid analysis of histamine in fishes (Fig. 4C). The mechanism of this method is that diamine oxidase catalyzed the hydrolysis of histamine to generate  $\text{H}_2\text{O}_2$ . Then, with the help of  $\text{MoO}_4^{2-}$ , the oxidation of  $\text{I}^-$  by  $\text{H}_2\text{O}_2$  produced  $\text{I}_2$ , which efficiently etched AuNRs, causing significant color changes in the detection solution. It was easy to differentiate with the naked eyes whether the detected histamine in a fish sample exceeded the maximum permissible limit of 50 mg/kg. Later, to enhance the activity of diamine oxidase, the same research group fixed it on magnetic graphene oxide [61]. This study found that the immobilized enzyme toward histamine was more sensitive than that of free enzymes.

Immunoassay based on specific antibody-antigen recognition has been demonstrated to be a promising technology for determining food safety due to its high sensitivity, excellent specificity, as well as high-throughput. Luo and coworkers [62] prepared tyramine specific monoclonal antibody for the establishment of a multicolor colorimetric ELISA for tyramine detection. The ALP labeled on the second antibody mediated the metallization of AuNSs, resulting in a series of color changes in response to different concentrations of tyramine. Besides, the quantitative determination of tyramine levels was

accomplished by analyzing the red and blue channel values in the detection solution images captured by a smartphone. This method was successfully applied to determine the freshness of beef, pork, and yogurt. The LOD of this method was 19.7 mg/kg. To improve the reliability and accuracy of detection results, Luo et al. [63] developed a dual-mode signal readout ELISA for histamine. On the one hand, this method also adopted the ALP mediated metallization of AuNRs strategy to obtain the colorimetric signal output. On the other hand, they used AuNRs as fluorescence quencher for carbon dots and regulated the fluorescence quenching ability of AuNRs through their morphological changes. As for multi-color colorimetric assay, a visible LOD of 0.25 mg/L was obtained; as for fluorescence assay, a LOD of 0.08 mg/L was obtained.

It should be noted that a major shortcoming of the above analysis methods is that their detection targets are limited to a single indicator, while the evaluation of food freshness demands simultaneous detection of multiple indicators. To overcome this issue, Orouji et al. [64] constructed a multicolor sensor array for the simultaneous determination of six types of biogenic amines based on biogenic amines mediated metallization of AuNRs and gold nanospheres. In this method, they employed partial least squares regression and linear discriminant analysis to qualitatively and quantitatively determine different biogenic amines. The accuracy of this sensor array for identifying biogenic amines in meat and fish samples was 98.92% and 99.67%, respectively. This method did not use biological enzymes, making it an economically effective and robust sensor. Thus, it was an ideal choice for practical applications. The above works indicate that gold nanomaterial-based multicolor colorimetric sensors have the advantages of easy operation, high throughput, high accuracy, and intuitive signal readout in the detection of food freshness indicators.

### 3.4. Pesticides

Pesticide refers to a substance or a mixture of substances and their formulations used to prevent and control diseases, insects, grass, mice, and other harmful organisms that harm agriculture and forestry, as well as to purposefully regulate the growth of plants and insects [65]. However, with the increasing abuse of pesticides in the agricultural field, pesticide residue pollution in food, natural water bodies, and even environmental soil poses a serious threat to food safety and public health [66]. Therefore, it is highly desirable to construct

appropriate methods to conveniently detect possible pesticide residues in real-world food samples.

Organophosphorus pesticides (OPs) refer to organic compound pesticides containing phosphorus elements. Although OPs can effectively prevent and control plant diseases, pests, and weeds, they exhibit high toxicity [67]. The toxic effect of OPs is mainly due to their phosphorylation of cholinesterase in the body, causing it to lose its ability to hydrolyze acetylcholine and leading to the accumulation of acetylcholine. Therefore, the development of sensitive methods for OPs is significant important for human health and environmental safety. Acetylthiocholine (ATCh), as a typical substrate of acetylcholinesterase (AChE), can be hydrolyzed by AChE to thiocholine (TCh). Specifically, TCh, as a molecule containing thiol, has strong binding ability with gold through Au–S bond. Liang et al. [68] innovatively developed a novel multicolor colorimetric sensor for OPs detection based on TCh regulation the *in situ* synthesis of AuNBPs. The increase in AChE concentration produces more TCh, leading to the gradual evolution of the shape of AuNBPs into cubes, finally forming

irregular spheres. As a result, OPs with inhibitory ability on AChE can be quantitatively analyzed by recording LSPR changes of the detection solution. The LODs toward paraoxon and demeton were 1.07 and 6.48 ng/mL, respectively. Besides, this method achieved the detection of paraoxon and demeton in citrus and cabbage with satisfactory results. On the other hand, molecules containing thiols have reducing properties, which can consume oxidants, thereby inhibiting their ability to etch gold nano-materials. Accordingly, Qing et al. [69] developed another multicolor colorimetric sensor for OPs detection (Fig. 5A). In the absence of OPs, AChE catalyzed the hydrolysis of acetylthiocholine iodide to TCh and  $I^-$ . The obtained TCh prevented the process of  $IO_3^-$  oxidation of  $I^-$  to form  $I_2$ , thereby inhibiting the etching of AuNRs. The presence of OPs inhibited the activity of AChE, allowing for the smooth generation of  $I_2$ , which in turn etched AuNRs, resulting in rich color changes in the solution. This method had a linear detection range of 0–117 nM for triazophos, with a LOD of 4.69 nM. Moreover, it has been demonstrated good potential for application through the determination of

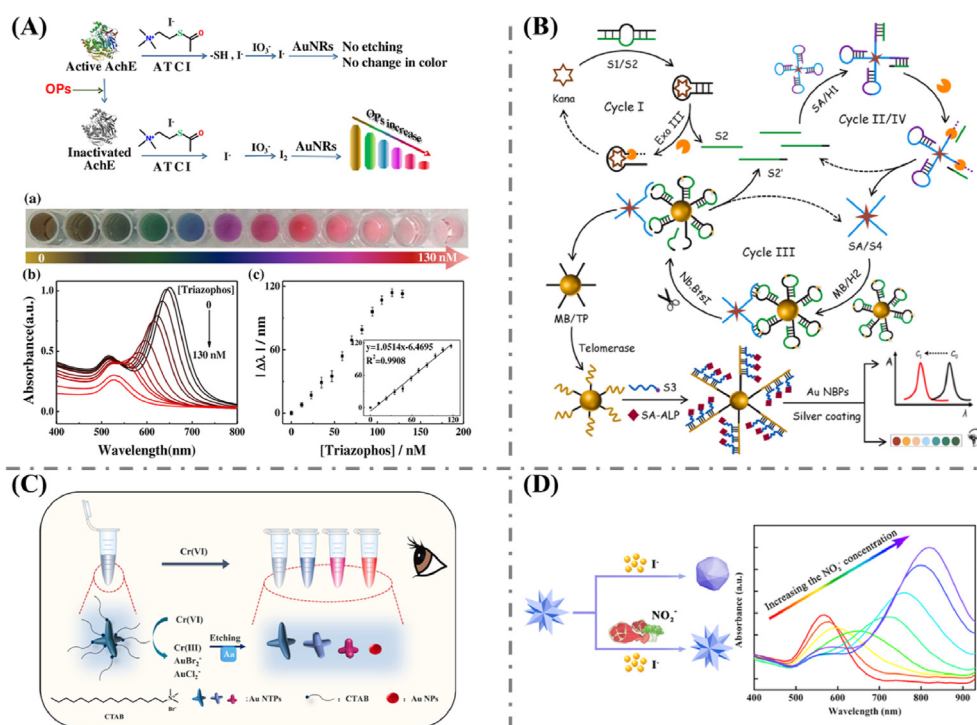


Fig. 5. Multicolor colorimetric sensors for the detection of chemical food hazards. (A) Schematic illustration of the multicolor colorimetric biosensor for the detection of OPs based on the etching of AuNRs by  $I_2$  (upper), and images (a), LSPR spectra (b), and LSPR peak shift (c) of the detection solution in response to different triazophos concentrations (lower). Reproduced with permission from Ref. [69]. (B) Schematic illustration of the multicolor colorimetric aptasensor for kanamycin determination in milk and honey based on ALP-mediated metallization of AuNBPs. Reproduced with permission from Ref. [86]. (C) Schematic illustration of the multicolor sensing platform for the detection of  $Cr^{6+}$  based on the etching of AuNTPs. Reproduced with permission from Ref. [94]. (D) Schematic illustration of the multicolor sensor for the detection of nitrite based on  $I_2$ -mediated etching of AuNSs. Reproduced with permission from Ref. [98].

triazophos in lake and tap water samples. To further improve the sensitivity, Liu et al. [70] developed a cascade catalytic reaction involving two enzymes to mediated the etching of AuNRs. The cascade reaction was initiated by converting acetylcholine chloride to choline through AChE. Subsequently, choline oxidase catalyzed the oxidation of choline to produce  $H_2O_2$ , leading to the etching of AuNRs. The presence of OPs inhibited the activity of AChE, thereby inhibiting the etching of AuNRs. This method achieved sensitive detection of dichlorvos and demeton, with LODs of 0.0081 and 0.32  $\mu\text{g/L}$ , respectively. In recent years,  $MnO_2$  nanosheets, as a type of nanozyme with good oxidase-like activity, have attracted extensive attention due to their ease of preparation, high stability, and good water solubility. Fu et al. [71] utilized AChE and  $MnO_2$  nanosheets to construct another dual enzyme cascade catalytic reaction to regulate the etching of AuNRs, achieving highly sensitive detection of OPs. The LOD for the detection of paraoxon was 11  $\text{ng/mL}$ .

In addition to AChE, researchers also utilized the characteristic of OPs inhibiting the activity of other enzymes to construct gold nanomaterial-based multicolor biosensors for the detection of OPs. For example, Chen et al. [72] designed a multicolor colorimetric method for the detection of OPs based on OPs induced inhibition of ascorbic acid oxidase (AAO) mediated metallization of AuNRs. The LOD of this method for trichlorfon was 132.6  $\text{ng/L}$ . Similarly, based on the inhibitory effect of OPs on ALP mediated metallization of AuNRs, Zhang et al. [73] developed another multicolor colorimetric method for the detection of omethoate in grape guice. The LOD of this method for omethoate was 94.10  $\text{ng/L}$ .

Additionally, many other pesticides also have the ability to inhibit enzyme activity. For example, 2,4-dichlorophenoxyacetic acid (2,4-D), a common herbicide, can inhibited the ALP activity. Ye et al. [74], prepared a paper-based analytical device for the quantitative detection of 2,4-D based on 2,4-D inhibition of ALP mediated *in situ* growth of AuNBPs (Fig. 5B). This method displayed seven colors related to the concentration of 2,4-D, with a LOD as low as 50  $\text{ng/mL}$  observed by the naked-eye and 18  $\text{ng/mL}$  recorded by a colorimeter. Nanozymes are increasingly favored by researchers due to their economic synthesis and storage stability. In fact, the activity of some nanozymes can also be inhibited by pesticides. Deng et al. [75] found that carbaryl can reduce the peroxidase activity of tetramethyl zinc (4-pyridinyl) porphyrin-dodecyl trimethylammonium bromide (ZnTPyP-DTAB), thereby inhibiting ZnTPyP-DTAB-mediated etching of AuNBPs. Based

on this principle, a high-resolution multicolor colorimetric biosensor for the detection of carbaryl was developed. The LOD of this method for carbaryl was 0.26  $\text{mg/kg}$ .

The multicolor colorimetric methods constructed above mainly relied on the impact of pesticides on enzyme activity. The involvement of enzymes increased the cost and operational steps to a certain extent. The dithiocarboxylic acid obtained by reducing disulfide bond groups of dithiocarbamates (DTCs) pesticides can form Au–S bonds with gold nanoparticles, thereby hindering the growth of AuNBPs. Based on this principle, Wang et al. [76] developed an enzyme free multicolor colorimetric sensor for the detection of DTCs in apple and black tea. The LOD observed by the naked eye was as low as 50  $\text{nM}$ , and the LOD measured by UV-visible spectroscopy was 17–18  $\text{nM}$ .

Moreover, to improve the specificity, Yin et al. [77] designed a multicolor colorimetric ELISA for the detection of OPs in cabbage, snow pear and rice.  $TMB^{2+}$  generated by HRP-ELISA effectively etched AuNRs, achieving high-resolution vivid color detection of OPs. The naked eye LOD was 0.25  $\text{ng/mL}$ . Based on a similar principle, Liu et al. [23] achieved a wide range detection of 0.08–100  $\text{ng/mL}$  for CBD. The multicolor ELISAs not only reserve the advantages of HRP-ELISA such as convenience, high specificity, and high sensitivity, but also overcome its drawbacks, that is, they can determine whether the pesticide in the sample exceeds the maximum residue limit (MRL) through visual observation without the help of large equipment.

### 3.5. Antibiotics

In recent years, antibiotic veterinary drugs have been extensively utilized for the prevention and treatment of diseases in livestock, fish, and bees, *etc.* With the increasing abuse of antibiotics, residue contamination of antibiotics in food poses a serious threat to food safety and public health [78]. Therefore, it is crucial to develop rapid and simple methods for the detection of antibiotics in food.

The sulfonamides (SAs), a longstanding class of synthetic antibiotics, have been extensively employed as feed supplements for treating infectious diseases in animal husbandry and aquaculture [79]. However, when animal husbandry excessively uses SAs, the residual SAs in animal derived foods inevitably becomes excessive. This may seriously endanger human health through the food chain. To ensure food safety, 100  $\mu\text{g/kg}$  is set by many governments as the MRL for total SAs in various food [80]. Therefore, the establishment of sensitive and

convenient SA detection methods is of great significance for human health. Earlier, Tian et al. [81] have demonstrated that  $\text{MnO}_2$  nanosheets with high oxidation ability can effectively etch AuNRs. Based on this feature, Fu's group [82] established a multicolor ELISA for the detection of six SAs by utilizing  $\text{MnO}_2$  nanosheets as oxidants to etch AuNBPs. This method exhibited a significant lower visual LOD for six different SAs (1–2  $\mu\text{g}/\text{kg}$ ) than the MRL value of the total SAs. When this method was used to detect SAs in milk, the recovery rates ranged from 84% to 106%. Later, the same group [83] developed another multicolor ELISA for the detection of five different SAs. The principle of this method is based on the *in situ* growth of AuNBPs mediated by ALP labeled on secondary antibody. HCl was added to regulate the growth rate of AuNBPs, thereby regulating the visual analysis sensitivity of the multicolor ELISA for SAs. A visual LOD of 0.1–0.5  $\text{ng}/\text{mL}$  was obtained under the condition of high concentration of HCl; while a visual LOD of 2–6  $\text{ng}/\text{mL}$  was obtained under the condition of low concentration of HCl. When this method was used to detect SAs in milk and fish muscle, the recovery rates ranged from 85% to 110%.

Kanamycin is an aminoglycoside antibiotic and an effective drug for preventing and treating microbial infections in humans and animals. However, the improper use of kanamycin can produce residues in animal derived foods, resulting in adverse effects on human health such as hearing loss, drug allergies, respiratory failure, nephrotoxicity, and ototoxicity through the food chain. To ensure food safety, the European Union has set a MRL of 100  $\mu\text{g}/\text{kg}$  for kanamycin in milk [84]. Compared with traditional antibodies, aptamers not only have the advantages of low cost, high affinity, good stability, non-toxicity, and easy synthesis, but also are easy to combine with various nucleic acid signal amplification technologies, which has great potential in constructing convenient and highly sensitive biosensors. For example, Yuwen et al. [85] developed a highly sensitive multicolor aptasensor for kanamycin determination by combining target-induced aptamer structure switch with cascade nucleic acid signal amplification technology. The binding between aptamer and kanamycin triggered toehold-mediated DNA-strand displacement reaction (SDA), enzymatic-mediated SDA, and HCR. The detection signal was generated by ALP-mediated metallization of AuNBPs, resulting in an ultra-low LOD of 1.4  $\text{fg}/\text{mL}$ . Later, the same group [86] developed another highly sensitive multicolor aptasensor for kanamycin determination in milk and honey by combining target-induced aptamer structure

transformation with a quadruple nucleic acid cycle strategy and telomerase-mediated DNA extension strategy (Fig. 5B). The binding between aptamer and kanamycin not only triggered target recycling (cycle I) induced by exonuclease III (Exo III), but also triggered the release of a strand, which participated in the following Exo III-driven DNA walking signal amplification (cycle II). The above reactions triggered a cascade DNA walker machine-based signal amplification reaction (cycle III) on MBs. This process, on the one hand, exposed the primers for telomerase elongation reaction; on the other hand, released another DNA to participate in the previous cycle (cycle IV). Due to the effectiveness of the established cascade signal amplification reaction, this method allowed for the detection of kanamycin as low as 17.6  $\text{fg}/\text{mL}$  within a wide linear range of five orders magnitude. Therefore, by applying various signal amplification strategies to the construction of multicolor colorimetric sensors significantly improves sensitivity, making then highly promising for on-site visual screening and accurate determination of antibiotic residues in the field of food safety monitoring.

### 3.6. Heavy metal ions

Currently, heavy metal ions are frequent contaminate drinking water and food. Due to the high toxicity, easy accumulation, and difficult degradation of heavy metal ions, they pose significant risks to human health and ecosystems. Therefore, it is highly vital to establish advanced sensors to accurately quantify of various heavy metal ions in food, drinking water, and the ecological environment. The currently established multicolor colorimetric sensors for heavy metal ions include  $\text{Ag}^+$ , mercury ion ( $\text{Hg}^{2+}$ ), chromium ion ( $\text{Cr}^{6+}$ ), and copper ion ( $\text{Cu}^{2+}$ ).

For example, Ma et al. [87] devised a multicolor colorimetric biosensor that relies on enzyme-mediated metallization of AuNRs for visual detection of  $\text{Hg}^{2+}$  in lake water samples. In this method, two thymine (T) rich DNA sequences were labelled with MBs and ALP, respectively. In the presence of  $\text{Hg}^{2+}$ , T rich DNA sequences recognized  $\text{Hg}^{2+}$  with high affinity and specificity by forming T- $\text{Hg}^{2+}$ -T complex [88]. This process resulted in ALP being attached to MBs. Subsequently, ALP mediated the metallization of AuNRs, resulting in a series of multicolored changes in response to different concentrations of  $\text{Hg}^{2+}$ . In addition, this method also achieved electrochemiluminescence detection of  $\text{Hg}^{2+}$ . This dual-model signal readout ensured more reliable and accurate detection results. Although

promising, this method requires complex modifications. To address this issue, Zhou et al. [89] developed a multicolor colorimetric method for  $\text{Cu}^{2+}$  detection, which was based on  $\text{Cu}^{2+}$ -creatinine nanozyme with peroxidase-like activity to mediate the etching of AuNRs. This method was simple and feasible, with a LOD of  $0.034 \mu\text{M}$  for  $\text{Cu}^{2+}$ . Moreover, it has been widely reported that heavy metal ions can significantly influence the enzymatic activity toward various enzymes. For example, Ma et al. [19] found out that  $\text{Ag}^+$  can significantly inhibit the PtNPs with catalase-like activity. This inhibitory effect facilitated a Fenton reaction between  $\text{H}_2\text{O}_2$  and  $\text{Fe}^{2+}$ , thereby promoting the etching of AuNRs and ultimately leading to multicolor changes in response to different concentrations of  $\text{Ag}^+$ . This method enabled naked-eye detection of  $\text{Ag}^+$  at  $800 \text{ nM}$ . Moreover, this method achieved good spiked recoveries in tap water and lake water testing.

In fact, different metals exhibit different redox potentials. For example, the standard electrode potential of  $\text{Hg}^{2+}/\text{Hg}^0$  ( $0.852 \text{ V}$ ) is higher than that of  $\text{Ag}^+/\text{Ag}^0$  ( $0.799 \text{ V}$ ), which means that  $\text{Hg}^{2+}$  can oxidize  $\text{Ag}^0$  to  $\text{Ag}^+$ . Based on this principle, Qi et al. [90] prepared  $\text{Ag}^0$  coated AuNBPs for the multicolor colorimetric detection of  $\text{Hg}^{2+}$ . By oxidizing  $\text{Ag}^0$  nanoshells on AuNBPs to  $\text{Ag}^+$  with  $\text{Hg}^{2+}$ , vivid colors corresponding to different concentrations of  $\text{Hg}^{2+}$  were observed. By visual observation, the LOD was as low as  $0.8 \mu\text{M}$ . In addition,  $\text{Cr}^{6+}$  can also oxidize  $\text{Ag}^0$ , thereby achieving etching of silver shells. For example, Kim et al. [91] wrapped a thick silver shell on the surface of AuNRs to construct a multicolor colorimetric sensor for  $\text{Cr}^{6+}$ . The detection range of  $\text{Cr}^{6+}$  could be adjusted by controlling the thickness of the silver nanoshell. This method showed a LOD of  $20 \text{ nM}$  for  $\text{Cr}^{6+}$ . Similarly, Liu et al. [92] developed another multicolor colorimetric sensor for  $\text{Cr}^{6+}$  based on  $\text{Cr}^{6+}$ -mediated etching of silver nanoshells on AuNBPs. Furthermore, Lu et al. [93] developed a similar multicolor colorimetric sensor for  $\text{Cu}^{2+}$ , as  $\text{Cu}^{2+}$  can also mediate the etching of silver nanoshells on AuNBPs. The LOD for naked eye detection was  $12 \mu\text{M}$ . It should be noted that under appropriate conditions,  $\text{Cr}^{6+}$  can also oxidate  $\text{Au}^0$ . For example, in the presence of  $\text{Br}^-$  or  $\text{Cl}^-$ , the electrode potential of  $\text{Cr}^{6+}/\text{Cr}^{3+}$  is higher than that of  $\text{Au}^+/\text{Au}^0$ . Based on this point, Wang et al. [94] first established a multicolor colorimetric sensor using gold nanotetrapods (AuNTPs) as chromogenic agents for the visualization detection of  $\text{Cr}^{6+}$  (Fig. 5C). The LOD of  $\text{Cr}^{6+}$  reached  $3 \text{ nM}$  for naked-eye detection. In addition, the method was tested on actual lake water samples

and showed good recovery rates. These results indicate that multicolor colorimetric sensors have important prospects in detecting harmful heavy metal ions to humans due to their intuitive signal readout, convenience, and cost-effectiveness.

### 3.7. Food additives

Due to the rapid development of the food industry, food additives have evolved into a crucial component of modern food industry. Food additives are substances added to processed food or other food products produced on an industrial scale for technical purposes, such as increasing food storage time, improving safety, and altering the sensory characteristics of food. Food additives that are allowed to be used, such as food seasoning agents, sweeteners, thickeners, *etc.*, can cause food safety issues when their use exceeds the standard requirement [95]. However, illegal food additives are not allowed to be used in food [96]. Therefore, the establishment of convenient and robust detection methods for qualitative and quantitative analysis of food additives is of great significance for food safety.

For example, as a food additive, nitrite helps maintain the fresh appearance of meat and exhibits strong reducibility and certain preservative effects. Excessive intake of nitrite can cause acute nitrite poisoning, resulting in methemoglobinemia, which can lead to tissue hypoxia and in severe cases, even death. In addition, long-term consumption of foods containing nitrite can lead to esophageal and gastric cancers [97]. Hong et al. [98] developed a multicolor colorimetric method for sensitively and selectively detection of nitrite in cabbage and sausage. The principle of this method is on the basis of the redox reaction between  $\text{I}^-$  and nitrite to regulate the etching of AuNSs (Fig. 5D). A low LOD of  $0.4 \mu\text{M}$  was obtained. In addition, by utilizing the oxidation ability of nitrite, Yoon et al. [99] developed another multicolor colorimetric method for visual detection of nitrite. This method is based on the direct etching of concave gold nanocubes by nitrite, which achieved sensitive detection of nitrite with a LOD of  $38 \text{ nM}$ . More importantly, this method exhibited a very fast response speed to nitrite, which can achieve the detection of nitrite in tap water and pond water within  $10 \text{ min}$ .

Due to its corrosion resistance properties, formaldehyde is often illegally added to food to extend its shelf life. For example, soaking food in formalin solution composed of 35%–40% formaldehyde can help improve food appearance. However, high levels of inhaled formaldehyde can irritate the eyes

and membranes, leading to cellular dysfunction and even carcinogenicity [100]. The International Agency for Research on Cancer has banned the use of formaldehyde as a food additive and listed it as a carcinogen. Therefore, the detection of formaldehyde in food has received high attention. Interestingly, formaldehyde with reducing ability can directly reduce  $\text{Ag}^+$  to  $\text{Ag}^0$ , thereby inducing the metallization of gold nanomaterials. By utilizing this strategy, Qi et al. [101] developed a multicolor colorimetric method based on gold nanoprisms for the sensitive detection of formaldehyde in octopus and chicken flesh. The linear range of this method was 0.1–100  $\mu\text{M}$ , with a LOD of 30 nM.

### 3.8. Hazards from food processing and packaging

Food processing is an important component of modern food industry. It enhances the color, aroma, taste, and preservation of food. However, hazardous substances such as advanced glycation end products, heterocyclic amines, methylimidazole, acrylamide, etc., may be produced during various processing steps, resulting in potential risks to consumer health [102]. For example, acrylamide is a potential human carcinogen. During high-temperature cooking (above 120 °C), due to the Maillard reaction, baked and fried foods are prone to produce acrylamide [103]. Therefore, the detection of acrylamide has attracted widespread attention. However, due to the lack of specific antibodies against acrylamide, constructing immunoassay methods toward acrylamide is challenging. To address this issue, Fu et al. [104] prepared a monoclonal antibody against xanthylacrylamide (XAA), which can be derived from acrylamide within 30 min at room temperature, to establish a multicolor ELISA for XAA. The amount of XAA was used to indirectly represent the concentration of acrylamide. The mechanism of this method was that ALP labeled on the antibody mediated the metallization of AuNRs. This method exhibited a linear range of 0.3–17.2 ng/mL, with a LOD of 0.06 ng/mL. Compared with conventional ELISA, the sensitivity was increased 3.6 times. The recovery rates obtained in instant noodles ranged from 84 to 102%. These results indicate that this multicolor colorimetric ELISA is a convenient and powerful screening method for monitoring the risk of acrylamide in various food samples.

In addition, due to the possibility of harmful substances in some packaging materials migrating into food, direct contact between food and packaging materials may cause chemical contamination. Dibutyl phthalate (DBP) used in the production of











polyvinyl chloride (PVC) can endow PVC with good flexibility. Due to the frequent use of PVC as a conveying pipeline in liquid food processing, the DBP of PVC may migrate into liquid food [105]. DBP can cause serious harm to human health, such as carcinogenesis, endocrine disruption, reproductive toxicity, and developmental toxicity. The European Union stipulates that infant food should not contain DBP, and the concentration of DBP migrated from food packaging materials to food should be less than 300  $\mu\text{g/L}$  [106]. Therefore, it is essential to construct a convenient and sensitive method for monitoring DBP in food samples. Huang et al. [107] proposed a competitive multicolor colorimetric ELISA for convenient and highly sensitive detection of DBP in liquor. This method involved the addition of AuNRs after the completion of the traditional HRP-ELISA, thus achieving multicolor colorimetric detection of DBP through  $\text{TMB}^{2+}$  induced etching of AuNRs. This method exhibited a linear range of 150–2700  $\mu\text{g/L}$ , with a LOD of 76 ng/L. The recovery rates obtained in *Erguotou* liquor ranged from 95.9 to 98.4%. The above methods demonstrate that the current multicolor colorimetric technology can provide fast, sensitive, and reliable outcomes for the detection of hazardous substances from food processing and packaging.

Table 1 shows the summary of the above-mentioned multicolor colorimetric biosensors (see Table 2).

## 4. Conclusion and outlook

The excellent physical and chemical properties of gold nanomaterials make them the preferred chromophore for constructing multicolor colorimetric sensors. This article reviewed the latest applications of advanced multicolor colorimetric sensors based on gold nanomaterials in the detection of food contaminants. We summarized the etching and growth strategies for constructing multicolor colorimetric sensors and discussed the principles for detecting different hazards in food in detail. These sensors are inexpensive, easy to handle, and convenient visualization, which are very helpful for low resource settings. However, there are still some limitations and challenges that need to be addressed before the widespread application. Firstly, it is crucial to synthesize gold nanomaterials with highly uniform morphology to achieve stable color display. However, the current methods for preparing gold nanomaterials cannot meet the requirements of large-scale applications. Secondly, there is a lack of theoretical calculations regarding the relationship between the color display of the solution and the

Table 1. Multicolor colorimetric sensors for food hazards based on gold nanomaterials.












Category	Tested target	Gold nanomaterial	Mechanism	Sensor readout	LOD	Dynamic range	Real sample	Visual color transition	Reference
Pathogens	<i>E. coli</i>	AuNRs	Etching	LSPR peak shift	22 CFU/mL	$1.0 \times 10^2$ – $1.0 \times 10^5$ CFU/mL	Apple juice, peach juice, water samples, orange juice, grape juice, urine, and river water		[30]
	<i>S. aureus</i>	AuNRs	Growth	Naked eyes	25 CFU/mL	/	Milk, urine, river water		[39]
	<i>S. aureus</i>	AuNBPs	Growth	LSPR peak shift	2.71 pM	10–100 pM and 100–600 pM	Milk		[41]
	<i>S. Choleraesuis</i>	AuNRs	Growth	LSPR peak shift	$1.21 \times 10^1$ CFU/mL	$10^1$ – $10^6$ CFU/mL	Whole milk		[42]
				Naked eyes	$1.21 \times 10^2$ CFU/mL	$1.21 \times 10^1$ – $1.21 \times 10^8$ CFU/mL			
	<i>L. monocytogenes</i>	AuNRs	Etching	LSPR peak shift	/	$10$ – $10^6$ CFU/mL	Pork		[44]
	<i>S. aureus</i>	AuNRs	Etching	LSPR peak shift	10 CFU/mL	$10$ – $10^6$ CFU/mL	Milk and pork		[45]
				Naked eyes	3.7 CFU/mL	/			
	<i>S. aureus</i>	AuNRs	Etching	LSPR peak shift	1.3 CFU/mL	$1.0 \times 10$ – $1.0 \times 10^6$ CFU/mL	Pork		[46]
	<i>L. monocytogenes</i>				1.2 CFU/mL	$1.0 \times 10$ – $1.0 \times 10^6$ CFU/mL			
	<i>E. coli</i> O157:H7				1.3 CFU/mL	$1.0 \times 10$ – $1.0 \times 10^6$ CFU/mL			
	<i>V. parahaemolyticus</i>				1.4 CFU/mL	$1.0 \times 10$ – $1.0 \times 10^6$ CFU/mL			
Above four pathogens				Naked eyes	10 CFU/mL	/			



Mycotoxins	ZEN	AuNSs	Etching	Naked eyes	0.1 ng/mL	/	Corn, wheat, and feed		[21]
				Smart phones RGB	0.07 ng/mL	0.07–2.54 ng/mL			
				UV-spectrum model	0.04 ng/mL	0.04–2.96 ng/mL			
	ZEN	AuNRs	Growth	Naked eyes	0.1 µg/L	/	/		[28]
				LSPR peak shift	/	0.001–100 µg/L			
	OTA	AuNFs	Growth	LSPR peak shift	8.205 pg/mL	5.0–640 pg/mL	Rice, corn, wheat, and wine		[29]
	AFB1	AuNRs	Etching	Naked eyes	0.12 ng/mL	/	Rice		[48]
	OTA	AuNRs	Etching	LSPR peak shift	0.83 ng/L	/	Millet and lake water		[50]
				Ratiometric fluorescence	0.56 ng/L	1 ng/L–10 µg/L			
				LSPR peak shift	5.7 pg/mL	0.01–10.0 ng/mL	Wheat flour		[51]
			LSPR peak shift	10 nM	10–200 nM	Beer		[52]	
			Naked eyes	30 nM	10 nM–1.0 µM				
			LSPR peak shift	9.0 nM	12.5–2 × 10 <sup>4</sup> nM	Grape juice		[53]	
			Photocurrent change	0.79 ng/L	1 ng/L–5 µg/L	/		[54]	
			LSPR peak shift	1.46 ng/L	1 ng/L–5 µg/L				
			LSPR peak shift	0.011 ng/mL	0.02–0.8 ng/mL	Cornmeal		[55]	
			Naked eyes	0.02 ng/mL	/				
			LSPR peak shift	57.93 ng/mL	0–2000 ng/mL	Wheat and maize		[56]	
			Naked eyes	1000 ng/mL	/				
			LSPR peak shift	0.47 ng/L	1 ng/L–5 µg/L	Millet		[57]	
			LSPR peak shift	13.36 µM	20–100 µM	Fish		[60]	
			Naked eyes	50 mg/kg	/				
			Absorbance values	11.39 µM	20–150 µM.				
			LSPR peak shift	1.23 µM	5–160 µM	Mackerel		[61]	
			Naked eyes	/	0–400 µM				
			Smartphone	0.246 mg/L	0.313–20 mg/L	Beef, pork, and yoghurt		[62]	
			R/B values	/					
			Naked eyes	/	0–40 mg/L				
			LSPR peak shift	0.2 mg/L	0.25–2.0 mg/L	Codfish and pork		[63]	
			Fluorescence intensity	0.08 mg/L	0.1–4.0 mg/L				
			Naked eyes	0.25 mg/L	0–10 mg/L				
			Absorbance values	14.26 µM	40–800 µM	Meat and fish	/	[64]	
				4.79 µM	20–800 µM				
				8.58 µM	40–800 µM				
				10.03 µM	60–800 µM				
				27.29 µM	80–800 µM				
				2.46 µM	10–800 µM				

(continued on next page)

Table 1. (continued)

Category	Tested target	Gold nanomaterial	Mechanism	Sensor readout	LOD	Dynamic range	Real sample	Visual color transition	Reference
Pesticides	Paraoxon	AuNBPs	Growth	Absorbance ratio	1.07 ng/mL	0–30 ng/mL	Citrus and cabbage		[68]
	Demeton				6.48 ng/mL	40–150 ng/mL			
	Triazophos	AuNRs	Etching	LSPR peak shift	4.69 nM	0–117 nM	Lake water and tap water		[69]
				Naked eyes	/	0–130 nM			
	Dichlorvos	AuNRs	Etching	LSPR peak shift	$0.81 \times 10^{-2}$ µg/L	0.01–50 µg/L	Water		[70]
	Demeton				0.32 µg/L	1.0–500 µg/L			
	Paraoxon	AuNRs	Etching	LSPR peak shift	11 ng/mL	80–600 ng/mL	/		[71]
	Trichlorfon	AuNRs	Growth	LSPR peak shift	132.6 ng/L	27.8–11111.1 µg/L	Lake water		[72]
	Omethoate	AuNRs	Etching	LSPR peak shift	83.2 ng/L	60–6000 µg/L	Tap water, river water, and grape juice		[73]
				Naked eyes	/	$20-1 \times 10^4$ µg/L			
	2,4-dichlorophenoxyacetic acid	AuNBPs	Etching	Colorimeter	18 ng/mL	0.05–1 µg/mL	Rice and apple		[74]
				Naked eyes	50 ng/mL	0–5 µg/mL			
	Carbaryl	AuNBPs	Etching	LSPR peak shift	0.26 mg/kg	0.8–8.0 mg/kg	Apple, cabbage, <i>Chrysanthemum morisfolium</i> , and <i>Lilium brownie</i>		[75]
				Naked eyes	2.5 mg/kg	0.8–8.0 mg/kg			
	Thiram	AuNBPs	Growth	LSPR peak shift	17 nM	0.02–1.2 µM	Apple and black tea		[76]
Ziram				17 nM	0.02–1.2 µM				
Zineb				18 nM	0.02–1.2 µM				
Thiram, ziram, and zineb				50 nM	0–15 µM				
Parathion-methyl	AuNRs	Etching	LSPR peak shift	2.42 ng/mL	$0.04-5 \mu\text{g mL}^{-1}$	Cabbage, snow pear, and rice		[77]	
Fenitrothion				0.95 pg/mL	$0.01-5 \mu\text{g mL}^{-1}$				
Parathion-methyl and fenitrothion				0.25 ng/mL	/				
Carbendazim	AuNRs	Etching	LSPR peak shift	0.25 ng/mL	0.08–20 ng/mL	Citrus, canned citrus, chives, and cabbage		[23]	
				0.49 ng/mL	/				

Antibiotics	Sulfamethazine	AuNBPs	Etching	LSPR peak shift Naked eyes	0.2 ng/mL 1 ng/mL	0–120 ng/mL /	Milk		[82]	
	Sulfamethazine	AuNBPs	Growth	LSPR peak shift	L- 0.40 ng/mL H- 5.00 fg/mL	1.0–18 ng/mL 0.06–1.5 ng/mL	Milk and fish		[83]	
	Sulfamethoxydiazine				L- 0.68 ng/mL H- 0.07 ng/mL	2.0–30 ng/mL 0.1–4.0 ng/mL				
	Sulfisomidine				L- 0.49 ng/mL H- 0.05 ng/mL	1.2–20 ng/mL 0.06–1.5 ng/mL				
	Sulfamerazine				L- 1.00 ng/mL H- 0.10 ng/mL	4.0–50 ng/mL 0.2–6.0 ng/mL				
	Sulfamonomethoxine				L- 1.47 ng/mL H- 0.16 ng/mL	7.0–50 ng/mL 0.5–10 ng/mL				
	Kanamycin	AuNBPs	Etching	LSPR peak shift Naked eyes	1.4 fg/mL /	10–1000 fg/mL 0–10 ng/mL	Milk and honey		[85]	
Heavy metal ions	Kanamycin	AuNBPs	Growth	LSPR peak shift Naked eyes	17.6 fg/mL /	0.1 pg/mL–10 ng/mL 0–100 ng/mL	Milk and honey		[86]	
	Hg <sup>2+</sup>	AuNRs	Growth	ECL intensity LSPR peak shift RGB values	0.32 pM 0.57 pM 1.12 pM	2 pM–500 nM 2 pM–500 nM 2 pM–500 nM	Lake water		[87]	
	Cu <sup>2+</sup>	AuNRs	Etching	LSPR peak shift Naked eyes	0.034 μM 0.5 μM	0.05–4.0 μM /	Lake water		[89]	
	Ag <sup>+</sup>	AuNRs	Etching	LSPR peak shift Naked eyes	8.0 nM 20 nM	0–500 nM /	Tap water and lake water		[19]	
	Hg <sup>2+</sup>	AuNBPs	Growth	LSPR peak shift Naked eyes	22 nM 0.8 μM	0.1–20 μM /	Tap water and lake water		[90]	
	Cr <sup>6+</sup>	AuNRs	Etching	LSPR peak shift	0.4 μM	2–60 μM	Tap water and pond water		[91]	
	Cr <sup>6+</sup>	AuNBPs	Etching	LSPR peak shift RGB values	1.69 μM 1.36 μM	2.5–40 μM 2.5–50 μM	Tap water and river water		[92]	
	Cu <sup>2+</sup>	AuNBPs	Etching	LSPR peak shift Naked eyes	0.16 μM 12 μM	4.0–100 μM /	Tap water and mineral water		[93]	
	Cr <sup>6+</sup>	AuNTPs	Etching	LSPR peak shift	0.5 nM	0.5–8 nM	Lake water		[94]	
	Food additives	Nitrite	AuNSs	Etching	Absorbance ratio	0.4 μM	2–300 μM	Cabbage and sausage		[98]
		Nitrite	Concave gold nanocubes	Etching	Absorbance ratio	38 nM	0.0–30 μM	Tap water and pond water		[99]
Formaldehyde		Gold nanoprism	Growth	Absorbance values RGB values	3 nM 30 nM	0.01–10 μM 0.1–100 μM	Octopus and chicken flesh		[101]	
Hazards from food processing and packaging	Acrylamide	AuNRs	Etching	LSPR peak shift Naked eyes	0.06 ng/mL 0.35 ng/mL	0.3–17.2 ng/mL 0–12.5 ng/mL	Instant noodles		[104]	
	Dibutyl phthalate	AuNRs	Etching	LSPR peak shift Naked eyes	76 ng/L 300 μg/L	150–2700 μg/L /	Erguotou liquor		[107]	

Note: The symbol “/” indicates information not provided or not applicable by the references. The abbreviation “H-” means high concentration of HCl and “L-” means low concentration of HCl.

Table 2. List of abbreviations.

Abbreviations	
AA	ascorbic acid
AAO	ascorbic acid oxidase
AAP	ascorbic acid 2-phosphate
AChE	acetylcholinesterase
AFB1	aflatoxin B1
Afs	aflatoxins
Ag <sup>+</sup>	silver ions
ALP	alkaline phosphatase
ATCh	acetylthiocholine
AuNBPs	gold nanobipyramids
AuNFs	gold nanoflowers
AuNRs	gold nanorods
AuNSs	gold nanostars
AuNTPs	gold nanotetrapods
BSA	bovine serum albumin
CBD	carbendazim
CTAB	cetyltrimethylammonium bromide
Cr <sup>6+</sup>	chromium ion
Cu <sup>2+</sup>	copper ion
DBP	dibutyl phthalate
DON	deoxynivalenol
DTCs	dithiocarbamates
<i>E. coli</i> O157:H7	<i>Escherichia coli</i> O157:H7
<i>E. coli</i>	<i>Escherichia coli</i>
ELISA	enzyme-linked immunosorbent assay
Exo I	exonuclease I
Exo III	exonuclease III
H <sub>2</sub> O <sub>2</sub>	hydrogen peroxide
HCRs	hybridization chain reactions
Hg <sup>2+</sup>	mercury ion
HRP	poly-horseradish peroxidase
I <sub>2</sub>	iodine
I <sup>-</sup>	iodide
<i>L. monocytogenes</i>	<i>Listeria monocytogenes</i>
LOD	limit of detection
LSPR	localized surface plasmon resonance
MBs	magnetic beads
Mnase	micrococcal nuclease
MnO <sub>2</sub> NPs	manganese dioxide nanoparticles
MRL	maximum residue limit
O <sub>2</sub>	oxygen
•OH	hydroxyl radicals
OPs	organophosphorus pesticides
OTA	ochratoxin A
PtNPs	platinum nanoparticles
PVC	polyvinyl chloride
<i>S. aureus</i>	<i>Staphylococcus aureus</i>
<i>S. Choleraesuis</i>	<i>Salmonella enterica Choleraesuis</i>
SAs	sulfonamides
SDA	strand displacement reaction
T	thymine
TCh	thiocholine
TMB	3,3',5,5'-tetramethylbenzidine
<i>V. parahaemolyticus</i>	<i>Vibrio parahaemolyticus</i>
XAA	xanthylacrylamide
ZEN	zearalenone
ZnTPyP-DTAB	tetramethyl zinc (4-pyridinyl) porphyrin-dodecyl trimethylammonium bromide
β-gal	beta-galactosidase
2,4-D	2,4-dichlorophenoxyacetic acid

morphology or composition of gold nanomaterials. In response to this issue, efforts should be made in the future through computer simulation. Thirdly, when analyzing real-world food samples, the interference of complex matrices on the morphological changes of gold nanomaterials remains a challenge. Fourthly, most multicolor colorimetric methods are developed in solution systems, so the convenience of use still needs to be improved.

Nevertheless, multicolor colorimetric sensors based on gold nanomaterials are a promising tool for rapid screening of food hazards. As research progresses further, we will witness the flourishing development of multicolor colorimetric sensors based on gold nanomaterials, which can be combined with mini-devices or smartphones to achieve more convenient and user-friendly detection of food hazards in the future.

### Declaration of competing interest

The authors declare that they have no conflicts of interest to this work.

### Acknowledgements

This work was financially supported by the Natural Science Foundation Project of CQ (No. cstc2021jcsj-msxmbX0819) and the Agriculture Research System of China (No. CARS-26).

### References

- [1] Zhou J, Liu Y, Du X, Gui Y, He J, Xie F, et al. Recent advances in design and application of nanomaterials-based colorimetric biosensors for agri-food safety analysis. *ACS Omega* 2023;8:46346–61.
- [2] Santovito E, Greco D, D'Ascanio V, Sanzani SM, Avantiaggiato G. Development of a DNA-based biosensor for the fast and sensitive detection of ochratoxin A in urine. *Anal Chim Acta* 2020;1133:20–9.
- [3] Satija J, Punjabi N, Mishra D, Mukherji S. Plasmonic-ELISA: expanding horizons. *RSC Adv* 2016;6:85440–56.
- [4] Wang F, Liu S, Lin M, Chen X, Lin S, Du X, et al. Colorimetric detection of microcystin-LR based on disassembly of orient-aggregated gold nanoparticle dimers. *Biosens Bioelectron* 2015;68:475–80.
- [5] Xu B, Xiang X, Ding Z, Luo Z, Huang J. A colorimetric assay for detection of glucose by enzymatic etching of triangular gold nanosheets. *Mater Chem Phys* 2023;301.
- [6] De A, Kalita D. Bio-fabricated gold and silver nanoparticle based plasmonic sensors for detection of environmental pollutants: an overview. *Crit Rev Anal Chem* 2021;53:672–88.
- [7] Guliy OI, Karavaeva OA, Smirnov AV, Eremin SA, Bunin VD. Optical sensors for bacterial detection. *Sensors (Basel)* 2023;23.
- [8] Tseng W-B, Hsieh M-M, Chen C-H, Chiu T-C, Tseng W-L. Functionalized gold nanoparticles for sensing of pesticides: a review. *J Food Drug Anal* 2020;28:522–39.

- [9] Liu D-M, Dong C. Gold nanoparticles as colorimetric probes in food analysis: progress and challenges. *Food Chem* 2023;429.
- [10] Zahra QuA, Luo Z, Ali R, Khan MI, Li F, Qiu B. Advances in gold nanoparticles-based colorimetric aptasensors for the detection of antibiotics: an overview of the past decade. *Nanomaterials (Basel)* 2021;11.
- [11] Sadiq Z, Safiabadi Tali SH, Hajimiri H, Al-Kassawneh M, Jahanshahi-Anbuhi S. Gold nanoparticles-based colorimetric assays for environmental monitoring and food safety evaluation. *Crit Rev Anal Chem* 2023;1–36.
- [12] Hua Z, Yu T, Liu D, Xianyu Y. Recent advances in gold nanoparticles-based biosensors for food safety detection. *Biosens Bioelectron* 2021;179.
- [13] Geleta GS. A colorimetric aptasensor based on gold nanoparticles for detection of microbial toxins: an alternative approach to conventional methods. *Anal Bioanal Chem* 2022;414:7103–22.
- [14] Manjubaashini N, Daniel Thangadurai T. Unaided-eye detection of diverse metal ions by AuNPs-based nanocomposites: a review. *Microchem J* 2023;190.
- [15] Xiong Y, Pei K, Wu Y, Duan H, Lai W, Xiong Y. Plasmonic ELISA based on enzyme-assisted etching of Au nanorods for the highly sensitive detection of aflatoxin B1 in corn samples. *Sens Actuators B Chem* 2018;267:320–7.
- [16] Shan G, Zheng S, Chen S, Chen Y, Liu Y. Detection of label-free H<sub>2</sub>O<sub>2</sub> based on sensitive Au nanorods as sensor. *Colloids Surf B Biointerfaces* 2013;102:327–30.
- [17] Chandrasekar G, Mougini K, Haidara H, Vidal L, Gnecco E. Shape and size transformation of gold nanorods (GNRs) via oxidation process: a reverse growth mechanism. *Appl Surf Sci* 2011;257:4175–9.
- [18] Kermanshahian K, Yadegar A, Ghourchian H. Gold nanorods etching as a powerful signaling process for plasmonic multicolorimetric chemo-/biosensors: strategies and applications. *Coord Chem Rev* 2021;442.
- [19] Ma X, Zhang H, Liu J, Zhang H, Hu X, Wang Y, et al. An ultrahigh-resolution multicolor sensing platform via target-induced etching of gold nanorods for multi-colorimetric analysis of trace silver ions. *Sens Actuators B Chem* 2023;397.
- [20] Xianyu Y, Lin Y, Chen Q, Belessiotis-Richards A, Stevens MM, Thomas MR. Iodide-mediated rapid and sensitive surface etching of gold nanostars for biosensing. *Angew Chem Int Ed* 2021;60:9891–6.
- [21] Lu W, Tian Y, Teng W, Qiu X, Li M. Plasmonic colorimetric immunosensor based on Poly-HRP and AuNS etching for tri-modal readout of small molecule. *Talanta* 2023;265.
- [22] Ma X, Lin Y, Guo L, Qiu B, Chen G, Yang H-h, et al. A universal multicolor immunosensor for semiquantitative visual detection of biomarkers with the naked eyes. *Biosens Bioelectron* 2017;87:122–8.
- [23] Liu H, Wang Y, Fu R, Zhou J, Liu Y, Zhao Q, et al. A multicolor enzyme-linked immunoassay method for visual readout of carbendazim. *Anal Methods* 2021;13:4256–65.
- [24] Priece P, Adekunle Salami H, Padilla RH, Zhong Z, Lopez-Sanchez JA. Anisotropic gold nanoparticles: preparation and applications in catalysis. *Chinese Journal of Catalysis* 2016;37:1619–50.
- [25] Gao Z, Deng K, Wang X-D, Miró M, Tang D. High-resolution colorimetric assay for rapid visual readout of phosphatase activity based on gold/silver core/shell nanorod. *ACS Appl Mater Interfaces* 2014;6:18243–50.
- [26] Hafez E, Moon B-S, Shaban SM, Pyun D-G, Kim D-H. Multicolor diagnosis of salivary alkaline phosphatase triggered by silver-coated gold nanobipyramids. *Microchim Acta* 2021;188.
- [27] Guo Y, Wu J, Li J, Ju H. A plasmonic colorimetric strategy for biosensing through enzyme guided growth of silver nanoparticles on gold nanostars. *Biosens Bioelectron* 2016; 78:267–73.
- [28] Ma T, Liu K, Yang X, Yang J, Pan M, Wang S. Development of indirect competitive ELISA and visualized multicolor ELISA based on gold nanorods growth for the determination of zearalenone. *Foods* 2021;10.
- [29] Pei K, Xiong Y, Xu B, Wu K, Li X, Jiang H, et al. Colorimetric ELISA for ochratoxin A detection based on the urease-induced metallization of gold nanoflowers. *Sens Actuators B Chem* 2018;262:102–9.
- [30] Zhou J, Tian F, Fu R, Yang Y, Jiao B, He Y. Enzyme-nanozyme cascade reaction-mediated etching of gold nanorods for the detection of *Escherichia coli*. *ACS Appl Nano Mater* 2020;3:9016–25.
- [31] Ghosh S, Manna L. The many “facets” of halide ions in the chemistry of colloidal inorganic nanocrystals. *Chem Rev* 2018;118:7804–64.
- [32] Park K, Drummy LF, Vaia RA. Ag shell morphology on Au nanorod core: role of Ag precursor complex. *J Mater Chem* 2011;21.
- [33] Chen J, Jackson AA, Rotello VM, Nugen SR. Colorimetric detection of *Escherichia coli* based on the enzyme-induced metallization of gold nanorods. *Small* 2016;12:2469–75.
- [34] Lohse SE, Burrows ND, Scarabelli L, Liz-Marzán LM, Murphy CJ. Anisotropic noble metal nanocrystal growth: the role of halides. *Chem Mater* 2013;26:34–43.
- [35] Lee J-H, Gibson KJ, Chen G, Weizmann Y. Bipyramid-templated synthesis of monodisperse anisotropic gold nanocrystals. *Nat Commun* 2015;6.
- [36] Wang Y, Xie L, Ma L, Wu Q, Li Z, Liu Y, et al. Ascorbic acid-mediated in situ growth of gold nanostars for photothermal immunoassay of ochratoxin A. *Food Chem* 2023;419.
- [37] Wang Y, Ma L, Xie L, Wu Q, Liu Y, Zhao Q, et al. Gold nanobipyramid-based photothermal immunoassay for portable detection of ochratoxin A in maize and grape juice. *ACS Appl Nano Mater* 2023;6:17858–68.
- [38] Wang Y, Liu Y, Wu Q, Fu R, Liu H, Cui Y, et al. Seed-mediated in situ growth of photothermal reagent gold nanostars: mechanism study and preliminary assay application. *Anal Chim Acta* 2022;1231:340424.
- [39] Zhou J, Fu R, Tian F, Yang Y, Jiao B, He Y. Dual enzyme-induced Au–Ag alloy nanorods as colorful chromogenic substrates for sensitive detection of *Staphylococcus aureus*. *ACS Appl Bio Mater* 2020;3:6103–9.
- [40] Beam JE, Wagner NJ, Lu K-Y, Parsons JB, Fowler VG, Rowe SE, et al. Inflammation-mediated glucose limitation induces antibiotic tolerance in *Staphylococcus aureus*. *iScience* 2023;26.
- [41] Zhou J, Fu R, Liu H, Liu Y, Wang Y, Jiao B, et al. Integrating multiple hybridization chain reactions on gold nanoparticle and alkaline phosphatase-mediated in situ growth of gold nanobipyramids: an ultrasensitive and high color resolution colorimetric method to detect the mecA gene of *Staphylococcus aureus*. *J Hazard Mater* 2021;418.
- [42] Gao B, Chen X, Huang X, Pei K, Xiong Y, Wu Y, et al. Urease-induced metallization of gold nanorods for the sensitive detection of *Salmonella enterica* Choleraesuis through colorimetric ELISA. *J Dairy Sci* 2019;102:1997–2007.
- [43] Hou Y, Jia B, Sheng P, Liao X, Shi L, Fang L, et al. Aptasensors for mycotoxins in foods: recent advances and future trends. *Compr Rev Food Sci Food Saf* 2021;21:2032–73.
- [44] Liu Y, Wang J, Zhao C, Guo X, Song X, Zhao W, et al. A multicolorimetric assay for rapid detection of *Listeria monocytogenes* based on the etching of gold nanorods. *Anal Chim Acta* 2019;1048:154–60.
- [45] Liu Y, Sun M, Qiao W, Cong S, Zhang Y, Wang L, et al. Multicolor colorimetric visual detection of *Staphylococcus aureus* based on Fe<sub>3</sub>O<sub>4</sub>–Ag–MnO<sub>2</sub> composites nano-oxidative mimetic enzyme. *Anal Chim Acta* 2023;1239.
- [46] Zhang H, Liu Y, Yao S, Shang M, Zhao C, Li J, et al. A multicolor sensing system for simultaneous detection of four foodborne pathogenic bacteria based on Fe<sub>3</sub>O<sub>4</sub>/MnO<sub>2</sub> nanocomposites and the etching of gold nanorods. *Food Chem Toxicol* 2021;149.
- [47] Barac A. Mycotoxins and human disease. In: Presterl E, editor. *Clinically relevant mycoses: a practical approach*. Cham: Springer International Publishing; 2019. p. 213–25.
- [48] Ma X, Chen Z, Kannan P, Lin Z, Qiu B, Guo L. Gold nanorods as colorful chromogenic substrates for

semiquantitative detection of nucleic acids, proteins, and small molecules with the naked eye. *Anal Chem* 2016;88:3227–34.

- [49] Zhao F, Li M, Wang L, Wang M. A colorimetric sensor enabled with heterogeneous nanozymes with phosphatase-like activity for the residue analysis of methyl parathion. *Foods* 2023;12.
- [50] Zhu H, Cai Y, Qileng A, Quan Z, Zeng W, He K, et al. Template-assisted Cu<sub>2</sub>O@Fe(OH)<sub>3</sub> yolk-shell nanocages as biomimetic peroxidase: a multi-colorimetry and ratiometric fluorescence separated-type immunosensor for the detection of ochratoxin A. *J Hazard Mater* 2021;411.
- [51] He S, Huang Q, Zhang Y, Zhang H, Xu H, Li X, et al. Magnetic beads-based multicolor colorimetric immunoassay for ultrasensitive detection of aflatoxin B1. *Chin Chem Lett* 2021;32:1462–5.
- [52] Yu X, Lin Y, Wang X, Xu L, Wang Z, Fu F. Exonuclease-assisted multicolor aptasensor for visual detection of ochratoxin A based on G-quadruplex-hemin DNAzyme-mediated etching of gold nanorod. *Mikrochim Acta* 2018;185:259.
- [53] Tian F, Zhou J, Fu R, Cui Y, Zhao Q, Jiao B, et al. Multicolor colorimetric detection of ochratoxin A via structure-switching aptamer and enzyme-induced metallization of gold nanorods. *Food Chem* 2020;320.
- [54] Wei J, Chen H, Chen H, Cui Y, Qileng A, Qin W, et al. Multifunctional peroxidase-encapsulated nanoliposomes: bioetching-induced photoelectrometric and colorimetric immunoassay for broad-spectrum detection of ochratoxins. *ACS Appl Mater Interfaces* 2019;11:23832–9.
- [55] Zhang Q, Zhang X, Zhang G, Chen W, Wu S, Yang H, et al. Multicolor immunosensor for detection of zearalenone based on etching Au NBPs mediated by HRP. *J Food Compos Anal* 2023;115.
- [56] Guo R, Ji Y, Chen J, Ye J, Ni B, Li L, et al. Multicolor visual detection of deoxynivalenol in grain based on magnetic immunoassay and enzymatic etching of plasmonic gold nanobipyramids. *Toxins* 2023;15.
- [57] Zhu H, Liu C, Liu X, Quan Z, Liu W, Liu Y. A multi-colorimetric immunosensor for visual detection of ochratoxin A by mimetic enzyme etching of gold nanobipyramids. *Mikrochim Acta* 2021;1883:62.
- [58] Cao Y, Chen M, Li J, Liu W, Zhu H, Liu Y. Continuous monitoring of temperature and freshness in cold chain transport based on the dual-responsive fluorescent hydrogel. *Food Chem* 2024;438.
- [59] Verma N, Hooda V, Gahlaut A, Gothwal A, Hooda V. Enzymatic biosensors for the quantification of biogenic amines: a literature update. *Crit Rev Biotechnol* 2019;40:1–14.
- [60] Xu X, Wu X, Ding Y, Zhou X. Multicolorimetric sensing of histamine in fishes based on enzymatic etching of gold nanorods. *Food Control* 2021;127.
- [61] Xu X, Wu X, Zhuang S, Zhang Y, Ding Y, Zhou X. Colorimetric biosensor based on magnetic enzyme and gold nanorods for visual detection of fish freshness. *Biosensors* 2022;12.
- [62] Luo L, Luo S-Z, Jia B-Z, Zhang W-F, Wang H, Wei X-Q, et al. A high-resolution colorimetric immunoassay for tyramine detection based on enzyme-enabled growth of gold nanostar coupled with smartphone readout. *Food Chem* 2022;396.
- [63] Luo S-Z, Yang J-Y, Jia B-Z, Wang H, Chen Z-J, Wei X-Q, et al. Multicolorimetric and fluorometric dual-modal immunosensor for histamine via enzyme-enabled metallization of gold nanorods and inner filter effect of carbon dots. *Food Control* 2022;137.
- [64] Orouji A, Ghasemi F, Bigdeli A, Hormozi-Nezhad MR. Providing multicolor plasmonic patterns with Au@Ag core-shell nanostructures for visual discrimination of biogenic amines. *ACS Appl Mater Interfaces* 2021;13:20865–74.
- [65] Li T, Wang J, Zhu L, Li C, Chang Q, Xu W. Advanced screening and tailoring strategies of pesticide aptamer for constructing biosensor. *Crit Rev Food Sci Nutr* 2022;63:10974–94.
- [66] Richardson JR, Fitsanakis V, Westerink RHS, Kanthasamy AG. Neurotoxicity of pesticides. *Acta Neuropathol* 2019;138:343–62.
- [67] Karthick Rajan D, Mohan K, Rajarajeswaran J, Divya D, Thanigaivel S, Zhang S. Toxic effects of organophosphate pesticide monocrotophos in aquatic organisms: a review of challenges, regulations and future perspectives. *Environ Res* 2024;244.
- [68] Liang D, Wang Y, Ma L, Liu Y, Fu R, Liu H, et al. Controlled growth of gold nanobipyramids using thiocholine for plasmonic colorimetric detection of organophosphorus pesticides. *ACS Appl Nano Mater* 2022;5:16978–86.
- [69] Qing Z, Li Y, Li Y, Luo G, Hu J, Zou Z, et al. Thiol-suppressed I<sub>2</sub>-etching of AuNRs: acetylcholinesterase-mediated colorimetric detection of organophosphorus pesticides. *Microchim Acta* 2020;187.
- [70] Liu Y, Lv B, Liu A, Liang G, Yin L, Pu Y, et al. Multicolor sensor for organophosphorus pesticides determination based on the bi-enzyme catalytic etching of gold nanorods. *Sensor Actuator B Chem* 2018;265:675–81.
- [71] Fu R, Zhou J, Wang Y, Liu Y, Liu H, Yang Q, et al. Oxidase-like nanozyme-mediated altering of the aspect ratio of gold nanorods for breaking through H<sub>2</sub>O<sub>2</sub>-supported multicolor colorimetric assay: application in the detection of acetylcholinesterase activity and its inhibitors. *ACS Appl Bio Mater* 2021;4:3539–46.
- [72] Chen G-Y, Zhang C-Y, Yin S-J, Zhou H-Y, Tian T, Peng L-J, et al. Highly sensitive visual colorimetric sensor for trichlorfon detection based on the inhibition of metallization of gold nanorods. *Spectrochim Acta Mol Biomol Spectrosc* 2022;270.
- [73] Zhang Q, Yu Y, Yun X, Luo B, Jiang H, Chen C, et al. Multicolor colorimetric sensor for detection of omethoate based on the inhibition of the enzyme-induced metallization of gold nanorods. *ACS Appl Nano Mater* 2020;3:5212–9.
- [74] Ye X, Zhang F, Yang L, Yang W, Zhang L, Wang Z. Paper-based multicolor sensor for on-site quantitative detection of 2,4-dichlorophenoxyacetic acid based on alkaline phosphatase-mediated gold nanobipyramids growth and colorimeter-assisted method for quantifying color. *Talanta* 2022;245.
- [75] Deng G, Wang S, Chen H, Ren L, Liang K, Wei L, et al. Digital image colorimetry in combination with chemometrics for the detection of carbaryl based on the peroxidase-like activity of nanoporphyrins and the etching process of gold nanoparticles. *Food Chem* 2022;394.
- [76] Wang Z, Yang L, Ye X, Huang C, Yang W, Zhang L, et al. Multicolor visual screening of total dithiocarbamate pesticides in foods based on sulfhydryl-mediated growth of gold nanobipyramids. *Anal Chim Acta* 2020;1139:59–67.
- [77] Yin X-L, Liu YQ, Gu H-W, Zhang Q, Zhang ZW, Li H, et al. Multicolor enzyme-linked immunosorbent sensor for sensitive detection of organophosphorus pesticides based on TMB<sup>2+</sup>-mediated etching of gold nanorods. *Microchem J* 2021;168.
- [78] Huemer M, Mairpady Shambat S, Brugger SD, Zinkernagel AS. Antibiotic resistance and persistence—implications for human health and treatment perspectives. *EMBO Rep* 2020;21.
- [79] Zhou D, Tan M, Li Z, Minjarez R. Trends of novel functional nanomaterials for analysis of sulfonamide residues in food products. *J Food Process Preserv* 2023;2023:1–9.
- [80] Li S, Zhang C, Tang H-X, Gu Y, Guo A-J, Wang K, et al. Determination of 24 sulfonamide antibiotics in instant pastries by modified QuEChERS coupled with ultra performance liquid chromatography-tandem mass spectrometry. *J Food Drug Anal* 2023;31:73–84.

- [81] Tian F, Fu R, Zhou J, Cui Y, Zhang Y, Jiao B, et al. Manganese dioxide nanosheet-mediated etching of gold nanorods for a multicolor colorimetric assay of total antioxidant capacity. *Sensor Actuator B Chem* 2020;321.
- [82] Chen Q, Pan Y, Sun C, Wang Z, Wu Y, Fu F. A multicolor immunosensor for the visual detection of six sulfonamides based on manganese dioxide nanosheet-mediated etching of gold nanobipyramids. *Talanta* 2023;258.
- [83] Wang Z, Li X, Zhang F, Gao Y, Cheng J, Fu F. Regulating the growth rate of gold nanobipyramids via a HCl-NADH-Ascorbic acid system toward a dual-channel multicolor colorimetric immunoassay for simultaneously screening and detecting multiple sulfonamides. *Anal Chem* 2023;95:10438–47.
- [84] Zhang X, Wang J, Wu Q, Li L, Wang Y, Yang H. Determination of kanamycin by high performance liquid chromatography. *Molecules* 2019;24.
- [85] Yuwen X, Zeng Y, Ruan S, Li X, Lai G. Dual cascade nucleic acid recycling-amplified assembly of hyperbranched DNA nanostructures to construct a novel plasmonic colorimetric biosensing method. *Analyst* 2023;148:3632–40.
- [86] Wang X, Yuwen X, Lai S, Li X, Lai G. Enhancement of telomerase extension via quadruple nucleic acid recycling to develop a novel colorimetric biosensing method for kanamycin assay. *Anal Chim Acta* 2024;1287.
- [87] Ma Y, Yu Y, Mu X, Yu C, Zhou Y, Chen J, et al. Enzyme-induced multicolor colorimetric and electrochemiluminescence sensor with a smartphone for visual and selective detection of Hg<sup>2+</sup>. *J Hazard Mater* 2021;415.
- [88] Miyake Y, Togashi H, Tashiro M, Yamaguchi H, Oda S, Kudo M, et al. MercuryII-mediated formation of Thymine–HgII–Thymine base pairs in DNA duplexes. *J Am Chem Soc* 2006;128:2172–3.
- [89] Zhou H-Y, Peng L-J, Tian T, Zhang W-Y, Chen G-Y, Zhang H, et al. Multicolor colorimetric assay for copper ion detection based on the etching of gold nanorods. *Microchim Acta* 2022;189.
- [90] Qi Y, Zhao J, Weng G, Li J, Zhu J, Zhao J. Modification-free colorimetric and visual detection of Hg<sup>2+</sup> based on the etching from core-shell structural Au-Ag nanorods to nanorices. *Sensor Actuator B Chem* 2018;267:181–90.
- [91] Kim D, Choi E, Lee C, Choi Y, Kim H, Yu T, et al. Highly sensitive and selective visual detection of Cr(VI) ions based on etching of silver-coated gold nanorods. *Nano Convergence* 2019;6.
- [92] Liu S, Wang X, Zou C, Zhou J, Yang M, Zhang S, et al. Colorimetric detection of Cr<sup>6+</sup> ions based on surface plasma resonance using the catalytic etching of gold nanodouble cone @ silver nanorods. *Anal Chim Acta* 2021;1149.
- [93] Lu M, Fu X, Xie H, Liu M, Wei P, Zhang W, et al. Colorimetric determination of copper ion based on the silver-coated gold nanobipyramids. *J Food Compos Anal* 2023;120.
- [94] Wang S, Shi Y, Zhang H, Sun Y, Wang F, Zeng L, et al. Colorimetric sensor for Cr (VI) by oxidative etching of gold nanotetrapods at room temperature. *Spectrochim Acta Mol Biomol Spectrosc* 2023;295.
- [95] Sepahvand M, Ghasemi F, Seyed Hosseini HM. Plasmonic nanoparticles for colorimetric detection of nitrite and nitrate. *Food Chem Toxicol* 2021;149.
- [96] Rahman MB, Hussain M, Kabiraz MP, Nordin N, Siddiqui SA, Bhowmik S, et al. An update on formaldehyde adulteration in food: sources, detection, mechanisms, and risk assessment. *Food Chem* 2023;427.
- [97] Shakil MH, Trisha AT, Rahman M, Talukdar S, Kobun R, Huda N, et al. Nitrites in cured meats, health risk issues, alternatives to nitrites: a review. *Foods* 2022;11.
- [98] Hong C, Li D, Cao S, Huang X, Yang H, Yang D, et al. Sensitive and multicolor detection of nitrite based on iodide-mediated etching of gold nanostars. *Chem Commun* 2022;58:12983–6.
- [99] Yoon S-J, Nam Y-S, Lee JY, Kim JY, Lee Y, Lee K-B. Highly sensitive colorimetric determination of nitrite based on the selective etching of concave gold nanocubes. *Microchim Acta* 2021;188.
- [100] Fappiano L, Carriera F, Iannone A, Notardonato I, Avino P. A review on recent sensing methods for determining formaldehyde in agri-food chain: a comparison with the conventional analytical approaches. *Foods* 2022;11.
- [101] Qi T, Xu M, Yao Y, Chen W, Xu M, Tang S, et al. Gold nanoprism/Tollens' reagent complex as plasmonic sensor in headspace single-drop microextraction for colorimetric detection of formaldehyde in food samples using smartphone readout. *Talanta* 2020;220.
- [102] Su D, Chen J, Du S, Kim H, Yu B, Wong KE, et al. Metabolomic markers of ultra-processed food and incident CKD. *Clin J Am Soc Nephrol* 2023;18:327–36.
- [103] Wang L, Liu Y, Gao H, Ge S, Yao X, Liu C, et al. Chronotoxicity of acrylamide in mice fed a high-fat diet: the involvement of liver CYP2E1 upregulation and gut leakage. *Molecules* 2023;28.
- [104] Fu H-J, Luo L, Wang Y, Wang C-L, Wang H, Shen Y-D, et al. Enzyme-induced silver deposition on gold nanorods for naked-eye and smartphone detection of acrylamide in food. *ACS Appl Nano Mater* 2022;5:12915–25.
- [105] Li W, Zhang X, Zhang H, Zhang C, Chen Y, Li C, et al. A nanozymatic-mediated smartphone colorimetric sensing platform for the detection of dimethyl phthalate (DMP) and dibutyl phthalate (DBP). *Biosensors* 2023;13.
- [106] Lestido-Cardama A, Sendón R, Bustos J, Lomo ML, Losada PP, de Quirós ARB. Dietary exposure estimation to chemicals transferred from milk and dairy products packaging materials in Spanish child and adolescent population. *Foods* 2020;9.
- [107] Huang Y, Lin Y, Luo F, Wang P, Wang J, Qiu B, et al. Rapid detection of dibutyl phthalate in liquor by a semi-quantitative multicolor immunosensor with naked eyes as readout. *Anal Methods* 2019;11:524–9.